

Fig. 1. Detection of NES activity in CDC25B1. (A) Schematic figures of CDC25B1 and the three possible NES regions (I, II, and III) are shown. Region I was previously reported to be an NES of CDC25B3. Sequences of the additional possible NES regions are shown. The amino acids indicated by asterisks are hydrophobic amino acids frequently observed in an NES. We constructed three mutants with Leu to Ala mutations (highlighted) that should abrogate the NES activity of each possible NES region. The numbers in each possible NES sequence represent the amino acid number from the N-terminus of CDC25B1 itself and not FLAG-tagged CDC25B1. CDC25B1 and the NES mutants were expressed as N-terminal 2× FLAG-tagged proteins. (B) HEK293 cells expressing CDC25B1 protein after transfection were detected and quantified in three groups as follows. N > C: cells with CDC25B detected specifically primarily in nuclei. N < C: cells with CDC25B detected specifically primarily in cytoplasm. N = C: cells with CDC25B detected non-specifically and evenly throughout cells. Standard errors, indicated as bars along the y-axis, result from three independent determinations that counted more than 200 cells in each experiment. (C) The effects of LMB (20 ng/ml for 3 h) on the localization of possible-NES mutants were determined. Expressed wild-type or mutant CDC25B1 was fixed and detected with anti-FLAG antibody and then treated with anti-rabbit Alexa Fluor 549 antibody as described in Materials and methods. Nuclei were identified by staining with DAPI. (D) The schematic figure of the 2× FLAG-CDC25B1Δ76 mutant. (E) The cytoplasmic localization of CDC25B1 is abolished by the deletion of the N-terminal 76 amino acids.

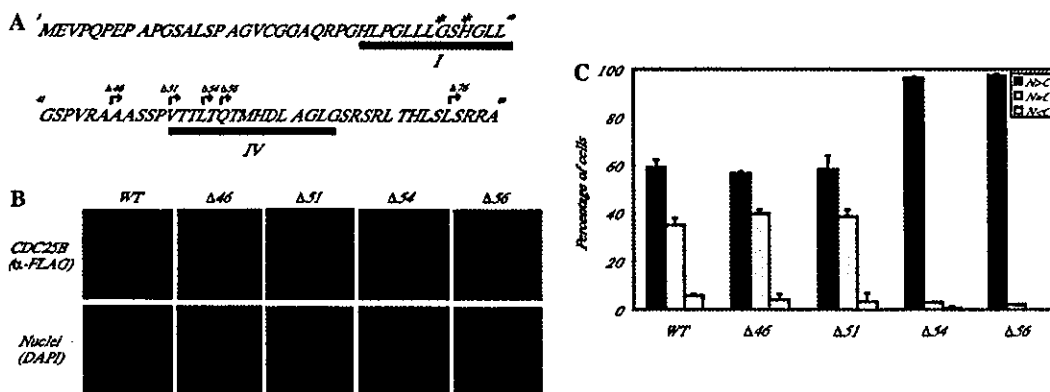


Fig. 2. Determination of the N-terminal boundary of the NES. (A) The sequence of the first N-terminal 80 amino acids is indicated. Underline I indicates the possible NES sequence previously reported. The amino acids marked with asterisks are those determined in a previous report to be essential for this NES activity. Underline IV is the NES sequence identified in this report. Δ46, Δ51, Δ54, Δ56, and Δ76 with arrows indicate the N-terminal ends of the N-terminal deletion mutants used in this experiment. These N-terminal deletion mutants were also expressed as N-terminal 2× FLAG-tagged proteins, as shown in Fig. 1A. (B) The subcellular localization of wild type or N-terminal deletion mutants was determined by transfection and detection of expressed proteins by indirect immunofluorescence as described in Materials and methods. (C) Percentages of cells expressing CDC25B1 protein primarily in nuclei (N > C), primarily in cytoplasm (N < C), or evenly distributed between both compartments (N = C) were quantified as described in the legend for Fig. 1D.

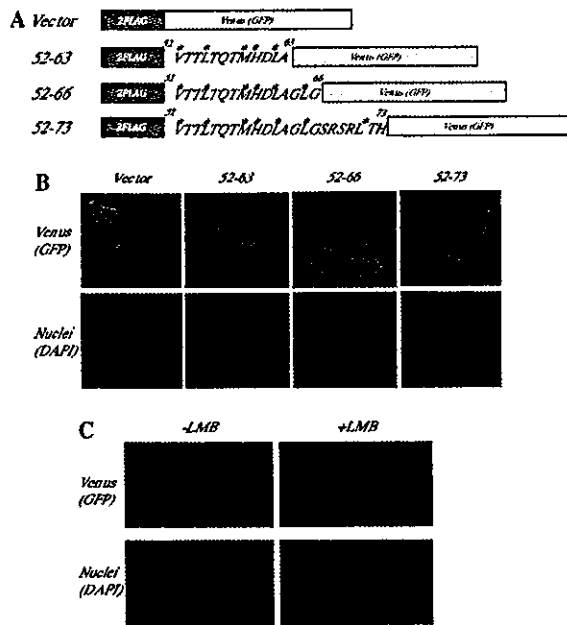


Fig. 3. Establishment of the minimum NES sequence of CDC25B. To determine the minimum NES sequence, oligonucleotides of several lengths starting at Val52 were designed and fused to Venus-GFP protein. (A) Schematic figures of the constructs are shown. Amino acids marked with asterisks are hydrophobic amino acids observed frequently in an NES. (B) Each plasmid was transfected into HEK293 cells and the localization of each GFP protein was determined. (C) To assess the effects of LMB on the GFP-fused NES, transfected cells were treated with 20 ng/ml LMB for 3 h and fixed, and the localization was determined. +LMB and –LMB indicate the results from cells with or without LMB treatment, respectively.

structurally similar residues such as Ile, Val, or Phe, that abort NES function when mutated [28]. The NES in CDC25B1 reporting here seems to include several potentially critical hydrophobic amino acids, Val52, Leu55, His60, Leu62, Leu65, and, less likely, Leu71.

It is important to determine if the amino acids between Val52 and Leu65 are essential to the NES of CDC25B1. To address this, the following CDC25B1 clones with different mutations in the suspected NES sequence were constructed: Val52 to Ala (denoted V52A), Leu55 to Ala (L55A), His60, Leu62, and Leu65 to Ala (H60AAA), and Leu71 to Ala (L71A) (Fig. 4A). The mutant CDC25B1 clones were expressed with FLAG-tags at the N-termini and their localizations were examined. Dramatic differences in the localization of the mutants were observed as shown in Fig. 4B. The mutation at Val52 abolished cytoplasmic localization, while that at Leu71 did not (Figs. 4B and C). Therefore, the NES of CDC25B1 starts at Val52 and ends before Leu71. Thus, the most important amino acid near the C-terminal end of the NES is Leu65. In addition, other mutants such as L55A and H60AAA with mutations in internal hydrophobic residues exhibited clear nuclear localization (Figs. 4B and C). Essentially the same

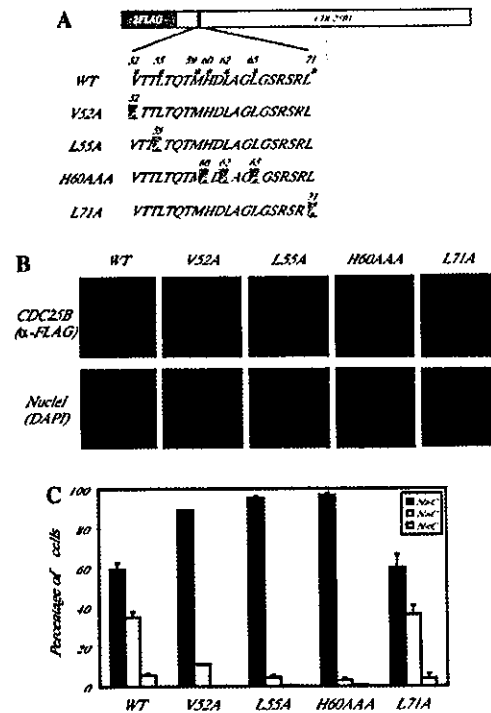


Fig. 4. Ablation of cytoplasmic localization of CDC25B1 by the introduction of mutations in the NES. Mutations were introduced at the possible critical amino acids in the NES region of N-terminally FLAG-tagged CDC25B1. (A) Schematic figures of mutated sequences of each mutant are indicated. Hydrophobic amino acids are marked with asterisks, and mutated amino acids, Ala, are highlighted. (B) Wild-type or mutant CDC25B1 plasmids were transfected into HEK293, and the expressed CDC25B1 proteins were detected by indirect immunofluorescence with anti-FLAG antibody and anti-rabbit Alexa Fluor 549. (C) The percentages of cells expressing CDC25B1 with a nuclear, diffuse, or cytoplasmic distribution were determined as shown in Fig. 1D.

results were obtained with Venus-GFP-fused fragments although NES-defective constructs did not exhibit specific localization in cells because of the lack of NLS sequence in Venus-GFP (data not shown). Therefore, we concluded that the amino acid sequence from Val52 to Leu65 of CDC25B1 is a functional NES in CDC25B1.

The subcellular localization of CDC25B is determined by the balance between NES and NLS activities and their modifiers, such as NES phosphorylation or 14-3-3 binding. On roles of 14-3-3 binding to CDC25B, there is much evidence that the binding masks the NLS located just downstream from the 14-3-3 binding site, tipping the balance in favor of the NES overriding the NLS. The proper cytoplasmic localization of target proteins with NES sequences seems to require both NES and 14-3-3 binding for *Xenopus* CDC25C and FKRL1 [26,29]. CDC25B also seems to be the case based on our results. The loss of 14-3-3 binding due to the mutation of a specific serine residue to alanine resulted in nuclear localization in CDC25B. Since a single NES domain from CDC25B can translocate GFP to the cytoplasm in

the absence of an NLS, the NLS in CDC25B would have to be stronger than the NES to keep the protein in the nucleus. Therefore, it is reasonable to conclude that both NES and 14-3-3 binding must be necessary to allow CDC25B to be exported from the nucleus to the cytoplasm. This is in clear contrast to human CDC25C in which the mutation of Ser216 to Ala at the 14-3-3 binding site does not completely abolish its cytoplasmic localization [30,31].

The significance of the cytoplasmic retention of CDC25 at the G2/M checkpoint requires a more thorough examination. In *Xenopus* or fission yeast, the ablation of 14-3-3 binding accelerates mitotic entry or erases cell cycle arrest due to DNA damage [32–34]. It is also reported that Ser309 of human CDC25B must be kept phosphorylated in order to exert proper G2 checkpoint [21,35]. These results strongly support the idea that 14-3-3 binding is necessary for G2 arrest following DNA damage. They do not, however, directly indicate that the cytoplasmic localization of CDC25 is essential for G2 arrest. In experiments with fission yeast, the necessity for the cytoplasmic retention of CDC25 at the DNA damage checkpoint was negated [36]. In addition, there are reports that phosphorylation of the 14-3-3 binding site in CDC25 directly inhibits its phosphatase activity [37] and that 14-3-3 binding inhibits the phosphatase activity of CDC25B [21,38]. Therefore, more experiments to assess the role of the cytoplasmic localization of CDC25B at the G2 DNA-damage checkpoint.

Acknowledgments

We thank H. Okayama (University of Tokyo) and A. Miyawaki (RIKEN) for the generous gifts of CDC25B1 cDNA and Venus, a modified GFP expression plasmid, respectively. This work was supported in part by Grants-in-Aid for Scientific Research (to K.Y. and Y.I.) and for the Second Term of the Comprehensive 10-Year Strategy for Cancer Control (to H.N.) from the Ministry of Health, Labor, and Welfare and by Grants-in-Aid of Scientific Research from the Japan Society for the Promotion of Science, the Ministry of Education, Science, Sports and Culture of Japan (to M.H. and T.M.).

References

- [1] D.O. Morgan, Cyclin-dependent kinases: engines, clocks, and microprocessors, *Annu. Rev. Cell. Dev. Biol.* 13 (1997) 261–291.
- [2] I. Nilsson, I. Hoffmann, Cell cycle regulation by the Cdc25 phosphatase family, *Prog. Cell Cycle Res.* 4 (2000) 107–114.
- [3] V. Baldin, C. Cans, G. Superti-Furga, B. Ducommun, Alternative splicing of the human CDC25B tyrosine phosphatase. Possible implications for growth control?, *Oncogene* 14 (1997) 2485–2495.
- [4] I. Hoffmann, G. Draetta, E. Karsenti, Activation of the phosphatase activity of human cdc25A by a cdk2–cyclin E dependent phosphorylation at the G1/S transition, *EMBO J.* 13 (1994) 4302–4310.
- [5] N. Mailand, A.V. Podtelejnikov, A. Groth, M. Mann, J. Bartek, J. Lukas, Regulation of G(2)/M events by Cdc25A through phosphorylation-dependent modulation of its stability, *EMBO J.* 21 (2002) 5911–5920.
- [6] J.P. Chow, W.Y. Siu, H.T. Ho, K.H. Ma, C.C. Ho, R.Y. Poon, Differential contribution of inhibitory phosphorylation of CDC2 and CDK2 for unperturbed cell cycle control and DNA integrity checkpoints, *J. Biol. Chem.* 278 (2003) 40815–40828.
- [7] M. Donzelli, G.F. Draetta, Regulating mammalian checkpoints through Cdc25 inactivation, *EMBO Rep.* 4 (2003) 671–677.
- [8] M.S. Chen, J. Hurov, L.S. White, T. Woodford-Thomas, H. Piwnica-Worms, Absence of apparent phenotype in mice lacking Cdc25C protein phosphatase, *Mol. Cell. Biol.* 21 (2001) 3853–3861.
- [9] A.J. Lincoln, D. Wickramasinghe, P. Stein, R.M. Schultz, M.E. Palko, M.P. De Miguel, L. Tessarollo, P.J. Donovan, Cdc25b phosphatase is required for resumption of meiosis during oocyte maturation, *Nat. Genet.* 30 (2002) 446–449.
- [10] K. Galaktionov, A.K. Lee, J. Eckstein, G. Draetta, J. Meckler, M. Loda, D. Beach, CDC25 phosphatases as potential human oncogenes, *Science* 269 (1995) 1575–1577.
- [11] D. Gasparotto, R. Maestro, S. Piccinin, T. Vukosavljevic, L. Barzan, S. Sulfaro, M. Boiocchi, Overexpression of CDC25A and CDC25B in head and neck cancers, *Cancer Res.* 57 (1997) 2366–2368.
- [12] S. Hernandez, L. Hernandez, S. Bea, M. Cazorla, P.L. Fernandez, A. Nadal, J. Muntane, C. Mallofre, E. Montserrat, A. Cardesa, E. Campo, cdc25 cell cycle-activating phosphatases and c-myc expression in human non-Hodgkin's lymphomas, *Cancer Res.* 58 (1998) 1762–1767.
- [13] W. Wu, Y.H. Fan, B.L. Kemp, G. Walsh, L. Mao, Overexpression of cdc25A and cdc25B is frequent in primary non-small cell lung cancer but is not associated with overexpression of c-myc, *Cancer Res.* 58 (1998) 4082–4085.
- [14] I. Takemasa, H. Yamamoto, M. Sekimoto, M. Ohue, S. Noura, Y. Miyake, T. Matsumoto, T. Aihara, N. Tomita, Y. Tamaki, I. Sakita, N. Kikkawa, N. Matsuura, H. Shiozaki, M. Monden, Overexpression of CDC25B phosphatase as a novel marker of poor prognosis of human colorectal carcinoma, *Cancer Res.* 60 (2000) 3043–3050.
- [15] H. Sasaki, H. Yukiue, Y. Kobayashi, M. Tanahashi, S. Moriyama, Y. Nakashima, I. Fukai, M. Kiriyama, Y. Yamakawa, Y. Fujii, Expression of the cdc25B gene as a prognosis marker in non-small cell lung cancer, *Cancer Lett.* 173 (2001) 187–192.
- [16] Z.Q. Ma, S.S. Chua, F.J. DeMayo, S.Y. Tsai, Induction of mammary gland hyperplasia in transgenic mice over-expressing human Cdc25B, *Oncogene* 18 (1999) 4564–4576.
- [17] Y. Yao, E.D. Slosberg, L. Wang, H. Hibshoosh, Y.J. Zhang, W.Q. Xing, R.M. Santella, I.B. Weinstein, Increased susceptibility to carcinogen-induced mammary tumors in MMTV-Cdc25B transgenic mice, *Oncogene* 18 (1999) 5159–5166.
- [18] C. Karlsson, S. Katich, A. Hagting, I. Hoffmann, J. Pines, Cdc25B and Cdc25C differ markedly in their properties as initiators of mitosis, *J. Cell Biol.* 146 (1999) 573–584.
- [19] H. Miyata, Y. Doki, H. Yamamoto, K. Kishi, H. Takemoto, Y. Fujiwara, T. Yasuda, M. Yano, M. Inoue, H. Shiozaki, I.B. Weinstein, M. Monden, Overexpression of CDC25B overrides radiation-induced G2-M arrest and results in increased apoptosis in esophageal cancer cells, *Cancer Res.* 61 (2001) 3188–3193.
- [20] N. Davezac, V. Baldin, B. Gabrielli, A. Forrest, N. Theis-Febvre, M. Yashida, B. Ducommun, Regulation of CDC25B phosphatases subcellular localization, *Oncogene* 19 (2000) 2179–2185.
- [21] A. Forrest, B. Gabrielli, Cdc25B activity is regulated by 14-3-3, *Oncogene* 20 (2001) 4393–4401.
- [22] K. Nishi, M. Yoshida, D. Fujiwara, M. Nishikawa, S. Horinouchi, T. Beppu, Leptomycin B targets a regulatory cascade of crml1, a fission yeast nuclear protein, involved in control of higher order chromosome structure and gene expression, *J. Biol. Chem.* 269 (1994) 6320–6324.

- [23] N. Kudo, B. Wolff, T. Sekimoto, E.P. Schreiner, Y. Yoneda, M. Yanagida, S. Horinouchi, M. Yoshida, Leptomycin B inhibition of signal-mediated nuclear export by direct binding to CRM1, *Exp. Cell. Res.* 242 (1998) 540–547.
- [24] Y. Wang, C. Jacobs, K.E. Hook, H. Duan, R.N. Booher, Y. Sun, Binding of 14-3-3beta to the carboxyl terminus of Wee1 increases Wee1 stability, kinase activity, and G2-M cell population, *Cell. Growth Differ.* 11 (2000) 211–219.
- [25] V. Mils, V. Baldin, F. Goubin, I. Pinta, C. Papin, M. Waye, A. Eychene, B. Ducommun, Specific interaction between 14-3-3 isoforms and the human CDC25B phosphatase, *Oncogene* 19 (2000) 1257–1265.
- [26] A. Kumagai, W.G. Dunphy, Binding of 14-3-3 proteins and nuclear export control the intracellular localization of the mitotic inducer Cdc25, *Genes Dev.* 13 (1999) 1067–1072.
- [27] T. Nagai, K. Ibata, E.S. Park, M. Kubota, K. Mikoshiba, A. Miyawaki, A variant of yellow fluorescent protein with fast and efficient maturation for cell-biological applications, *Nat. Biotechnol.* 20 (2002) 87–90.
- [28] M. Watanabe, N. Masuyama, M. Fukuda, E. Nishida, Regulation of intracellular dynamics of Smad4 by its leucine-rich nuclear export signal, *EMBO Rep.* 1 (2000) 176–182.
- [29] A. Brunet, F. Kanai, J. Stehn, J. Xu, D. Sarbassova, J.V. Frangioni, S.N. Dalal, J.A. DeCaprio, M.E. Greenberg, M.B. Yaffe, 14-3-3 transits to the nucleus and participates in dynamic nucleocytoplasmic transport, *J. Cell Biol.* 156 (2002) 817–828.
- [30] S.N. Dalal, C.M. Schweitzer, J. Gan, J.A. DeCaprio, Cytoplasmic localization of human cdc25C during interphase requires an intact 14-3-3 binding site, *Mol. Cell. Biol.* 19 (1999) 4465–4479.
- [31] P.R. Graves, C.M. Lovly, G.L. Uy, H. Piwnica-Worms, Localization of human Cdc25C is regulated both by nuclear export and 14-3-3 protein binding, *Oncogene* 20 (2001) 1839–1851.
- [32] A. Kumagai, P.S. Yakowec, W.G. Dunphy, 14-3-3 proteins act as negative regulators of the mitotic inducer Cdc25 in *Xenopus* egg extracts, *Mol. Biol. Cell* 9 (1998) 345–354.
- [33] J. Yang, K. Winkler, M. Yoshida, S. Kornbluth, Maintenance of G2 arrest in the *Xenopus* oocyte: a role for 14-3-3-mediated inhibition of Cdc25 nuclear import, *EMBO J.* 18 (1999) 2174–2183.
- [34] Y. Zeng, H. Piwnica-Worms, DNA damage and replication checkpoints in fission yeast require nuclear exclusion of the Cdc25 phosphatase via 14-3-3 binding, *Mol. Cell. Biol.* 19 (1999) 7410–7419.
- [35] D.V. Bulavin, Y. Higashimoto, I.J. Popoff, W.A. Gaarde, V. Basrur, O. Potapova, E. Appella, A.J. Fornace Jr., Initiation of a G2/M checkpoint after ultraviolet radiation requires p38 kinase, *Nature* 411 (2001) 102–107.
- [36] A. Lopez-Girona, B. Furnari, O. Mondesert, P. Russell, Nuclear localization of Cdc25 is regulated by DNA damage and a 14-3-3 protein, *Nature* 397 (1999) 172–175.
- [37] B. Furnari, A. Blasina, M.N. Boddy, C.H. McGowan, P. Russell, Cdc25 inhibited in vivo and in vitro by checkpoint kinases Cdk1 and Chk1, *Mol. Biol. Cell* 10 (1999) 833–845.
- [38] N. Giles, A. Forrest, B. Gabrielli, 14-3-3 acts as an intramolecular bridge to regulate cdc25B localization and activity, *J. Biol. Chem.* 278 (2003) 28580–28587.

Binding of 14-3-3 β but not 14-3-3 σ controls the cytoplasmic localization of CDC25B: binding site preferences of 14-3-3 subtypes and the subcellular localization of CDC25B

Sanae Uchida¹, Akiko Kuma^{1,*}, Motoaki Ohtsubo², Mari Shimura³, Masato Hirata⁴, Hitoshi Nakagama⁵, Tsukasa Matsunaga⁶, Yukihiro Ishizaka³ and Katsumi Yamashita^{1,‡}

¹Division of Life Science, Graduate School of Natural Science and Technology, Kanazawa University, Kakuma-machi, Kanazawa, 920-1192, Japan

²Institute of Life Science, Kurume University, Aikawa 2432-3, Kurume, 839-0861, Japan

³Division of Intractable Disease, International Medical Center of Japan, 21-1 Toyama 1-chome, Shinjuku-ku, Tokyo, 162-8655, Japan

⁴Laboratory of Molecular and Cellular Biochemistry, Faculty of Dental Science, and Station for Collaborative Research, Kyushu University, Maidashi, Fukuoka, 812-8582, Japan

⁵Biochemistry Division, National Cancer Center Research Institute, 1-1 Tsukiji 5-chome, Chuo-ku, Tokyo, 104-0045, Japan

⁶Laboratory of Molecular Human Genetics, Faculty of Pharmaceutical Sciences, Kanazawa University, 13-1 Takara-machi, Kanazawa, 920-0934, Japan

*Present address: Department of Cell Biology, National Institute for Basic Biology, 38 Nishigonaka, Myodaiji, Okazaki, 444-8585, Japan

‡Author for correspondence (e-mail: katsumi@kenroku.kanazawa-u.ac.jp)

Accepted 7 January 2004

Journal of Cell Science 117, 3011-3020 Published by The Company of Biologists 2004

doi:10.1242/jcs.01086

Summary

The dual specificity phosphatase CDC25B positively controls the G2-M transition by activating CDK1/cyclin B. The binding of 14-3-3 to CDC25B has been shown to regulate the subcellular redistribution of CDC25B from the nucleus to the cytoplasm and may be correlated with the G2 checkpoint. We used a FLAG-tagged version of CDC25B to study the differences among the binding sites for the 14-3-3 subtypes, 14-3-3 β , 14-3-3 ϵ and 14-3-3 σ , and the relationship between subtype binding and the subcellular localization of CDC25B. All three subtypes were found to bind to CDC25B. Site-directed mutagenesis studies revealed that 14-3-3 β bound exclusively near serine-309 of CDC25B1, which is within a potential consensus motif for 14-3-3 binding. By contrast, 14-3-3 σ bound preferentially to a site around serine-216, and the presence of serine-137 and -309 enhanced the binding. In addition to these binding-site differences, we found that the binding of 14-3-3 β drove CDC25B to the cytoplasm and that mutation

of serine-309 to alanine completely abolished the cytoplasmic localization of CDC25B. However, co-expression of 14-3-3 σ and CDC25B did not affect the subcellular localization of CDC25B. Furthermore, serine-309 of CDC25B was sufficient to produce its cytoplasmic distribution with co-expression of 14-3-3 β , even when other putative 14-3-3 binding sites were mutated. 14-3-3 ϵ resembled 14-3-3 β with regard to its binding to CDC25B and the control of CDC25B subcellular localization. The results of the present study indicate that two 14-3-3 subtypes can control the subcellular localization of CDC25B by binding to a specific site and that 14-3-3 σ has effects on CDC25B other than the control of its subcellular localization.

Key words: CDC25B, 14-3-3 β , 14-3-3 σ , Subcellular localization, G2 checkpoint

Introduction

The CDK (cyclin-dependent kinase) family of proteins controls the eukaryotic cell cycle, and one of these proteins, CDK1, is required for the onset and maintenance of mitosis. The activities of CDK family proteins related to cell cycle control are regulated by associations with cyclin proteins, interactions with cyclin-dependent kinase inhibitors, such as p21 and p27, and the phosphorylation-dephosphorylation cycle of CDK (Morgan, 1997). For instance, the phosphorylation of CDK1 at threonine-14 and tyrosine-15 by Wee1 and/or Myt1 kinases negatively controls CDK1 activity, whereas the dephosphorylation of CDK1 by the CDC25 family phosphatases activates CDK1, an essential step in the transition from G2 to M phase. The CDC25 family of dual protein

phosphatases consists of three members, CDC25A, CDC25B, and CDC25C (Nilsson and Hoffman, 2000). CDC25A is thought to regulate the G1 to S transition, and CDC25B and C have been proposed to activate the CDK1/cyclin B1 complex to advance the cell cycle from G2 to M. Recent reports strongly suggest that CDC25A also has a function that is essential for the entry into and maintenance of M phase (Mailand et al., 2002).

The 14-3-3 family of proteins consists of small, acidic, highly conserved proteins that are present in all eukaryotic cells from yeast to mammals. There are seven isoforms present in mammalian cells. The 14-3-3 proteins are involved in numerous cellular processes related to signal transduction (Muslin and Xing, 2000; Tzivion et al., 2001; Yaffe, 2002).

These molecules bind to phosphoproteins at specific sequence motifs, which contain phosphoserine/threonine residues three amino acids downstream of an arginine (RxxS/T), and thereby regulate extracellular signaling or stress response pathways (Muslin et al., 1996; Yaffe et al., 1997). Emerging evidence suggests that 14-3-3 proteins are key regulators of cell cycle control, especially at cell cycle checkpoints, where they might function as negative regulators of DNA damage checkpoints. For example, one canonical 14-3-3 binding motif, which contains a phosphorylated serine residue, is similar to the consensus substrate motif of the checkpoint kinase Chk1 (Sanchez et al., 1997; Hutchins et al., 2000). In fission yeast, the 14-3-3 proteins Rad24/25 are required for checkpoint responses and are essential for cell survival (Ford et al., 1994). One of the 14-3-3 isotype proteins, 14-3-3 σ is strongly up-regulated following genotoxic stress and is a downstream target of the tumor suppressor p53 (Hermeking et al., 1997).

The involvement of 14-3-3 in the progression from G2 to M was first suggested by the interactions of isolated 14-3-3 β and ϵ with CDC25B (and CDC25A) and of isolated 14-3-3 ζ with Wee1 (Conklin et al., 1995; Honda et al., 1997). Accumulated circumstantial evidence indicates that 14-3-3 negatively controls the G2-M transition by binding to these regulators. An association of 14-3-3 with human CDC25C was detected in G1, S and G2 phases, but not in M phase (Peng et al., 1997). The binding of 14-3-3 requires the Ser216 of CDC25C, and mutating this residue to Ala abolishes the interaction. This site is present in the potential recognition motif for 14-3-3 and is phosphorylated *in vitro* by checkpoint kinases, such as Chk1 and Chk2 (Sanchez et al., 1997; Peng et al., 1998; Matsuoka et al., 1998; O'Neill et al., 2002). Studies of the interaction between *Xenopus* CDC25C and 14-3-3 clearly demonstrated that the binding of 14-3-3 masks the nuclear localization signal of CDC25C, thereby causing nuclear exclusion of the protein without affecting its phosphatase activity (Kumagai et al., 1998; Kumagai and Dunphy, 1999; Yang et al., 1999). By contrast, the binding of 14-3-3 to *Xenopus* Wee1, after Chk1 activation by DNA damage or by stalled replication, augments Wee1 tyrosine kinase activity for CDK1 (Wang et al., 2000; Lee et al., 2001; Rothblum-Oviatt et al., 2001). Thus, the association of 14-3-3 with target proteins could modulate cell cycle progression through different mechanisms such as subcellular localization and enzyme activity, depending on cellular signaling.

In the normal cell cycle, CDC25B accumulates only at G2 phase and is degraded when cells exit M phase (Nagata et al., 1991; Galaktionov and Beach, 1991; Sebastian et al., 1993; Lammer et al., 1998). Interestingly, the overexpression of CDC25B induces a mitotic catastrophe by prematurely activating CDK1/cyclin B1, indicating that CDC25B induces mitosis more efficiently than CDC25C (Karlsson et al., 1999). In addition, the exogenous expression of CDC25B can override the G2 DNA damage checkpoint, and CDC25B is expressed in certain tumors (Miyata et al., 2001). Therefore, CDC25B has been proposed to be a potential oncogene acting to abrogate the DNA damage checkpoint (Galaktionov et al., 1995; Ma et al., 1999; Yao et al., 1999). Subcellular localization of CDC25B can be controlled by its association with 14-3-3 at a specific site on CDC25B2 or B3, Ser323 and might contribute to stall the cell cycle at the G2 phase following DNA damage (Mils et al., 2000; Davezac et al., 2000; Forrest and Babrielli, 2001). Ser323 of CDC25B2 or CDC25B3 (the equivalent to

Ser309 of CDC25B1) is a crucial residue in the consensus 14-3-3 binding motif, where it is phosphorylated by the stress kinase p38 (Bulavin et al., 2001).

In the present study, we have analyzed the binding site specificity of three 14-3-3 subtypes, 14-3-3 β , ϵ , and σ . Our results indicate that the binding site of 14-3-3 σ differs markedly from those of 14-3-3 β and 14-3-3 ϵ . Moreover, the interaction of 14-3-3 β or 14-3-3 ϵ , but not of 14-3-3 σ with CDC25B drives CDC25B from the nucleus into the cytoplasm. The biological significance of our results is discussed.

Materials and Methods

Cell culture and transfection

HEK293 cells (ATCC number CRL-1573) and U2OS cells (ATCC number HTB-96) were cultured in Dulbecco's modified Eagle's medium (DMEM) (Sigma, USA) supplemented with 10% fetal bovine serum (FBS) (Invitrogen, USA), 100 units/ml penicillin and 10 μ g/ml streptomycin. Transient transfections were performed with FuGENE6 (Roche Diagnostics, Germany). For immunoprecipitation, cells were typically seeded at 1.3×10^6 per well. After 24 hours, cells were co-transfected with 2.5 μ g of FLAG-tagged CDC25B and 1.0 μ g of myc-tagged 14-3-3 DNA. For the indirect immunofluorescence experiments, cells were plated at a lower density, 2.0×10^5 per well and transfected after 24 hours with 3.0 μ g of CDC25B DNA and 1.5 μ g 14-3-3 of DNA. Transfected cells were processed for immunoblotting, immunoprecipitation, or immunostaining 24 hours after transfection. Leptomycin B, an inhibitor of CRM1 (exportin1), was obtained from Minoru Yoshida (RIKEN, Wako, Japan) and was administered to cells at a dose of 20 ng/ml to induce the nuclear accumulation of CDC25B.

Plasmids and site-directed mutagenesis

The cDNA of human CDC25B (CDC25B1 subtype), a kind gift from H. Okayama (University of Tokyo, Japan), was subcloned into the pEF6B vector (Invitrogen, USA) and expressed in transfected cells with a C-terminal FLAG tag. For point mutations at putative 14-3-3 binding sites, the following oligonucleotides (and their complements) were used to change serine to alanine (SA) in human CDC25B cDNA (CDC25B1). Clones with multiple mutations were generated by exchanging restriction fragments. The mutations were confirmed by sequencing.

S81A: 5'-CTGTCTCGACGGGCAGCCGAATCCTCCCTG-3',
S137A: 5'-ATCAGACGCTTCCAGGCTATGCCGGTGAGG-3',
S216A: 5'-GCCAGAGACCCAGCGGCCCGCCCGACCTG-3',
S309A: 5'-CTCTTCCGCTCTCCGGCCATGCCCTGCAGC-3',
S361A: 5'-GTCCTCCGCTCAAAGCACTGTGTACAGAT-3'.

The cDNAs of human 14-3-3 β , ϵ , and σ were obtained by PCR amplification with the following oligonucleotides:

14-3-3 β forward: 5'-ACTTGGAGTCAGCATATGACAATGGAT-3',
14-3-3 β reverse: 5'-CACTGGACGGATCCCAAAGCACGAGAA-3',
14-3-3 ϵ forward: 5'-GCCGCTGCCCATATGGATGATCGAGAG-3',
14-3-3 ϵ reverse: 5'-CTCTTGTGGGCGGATCCCTCACTGATT-3',
14-3-3 σ forward: 5'-GTCCCAGACATATGGAGAGAGCCAGT-3',
14-3-3 σ reverse: 5'-GGTGGCGGGCAAGCTTCAGCTCTGGGG-CTC-3'.

PCR products were subcloned into the pEF6 vector. Each 14-3-3 cDNA was expressed in transfected cells in an N-terminal myc-tagged form.

Antibodies

Anti-FLAG M2 agarose was obtained from Sigma (USA). The rabbit

anti-FLAG antibody was described previously (Wang et al., 2001). Rabbit polyclonal and mouse monoclonal anti-myc-tag antibodies were purchased from Cell Signaling (USA). Antibodies to 14-3-3 β (C-20), 14-3-3 ϵ (T-16), and 14-3-3 σ (N-14) were purchased from Santa Cruz Biotechnology (USA).

Preparation of crude cell extracts, immunoprecipitation and immunoblotting

Transfected cells were lysed in immunoprecipitation (IP) buffer (50 mM Tris-HCl pH 7.5, 150 mM NaCl, 0.5% NP-40, 5 mM EGTA, 1 mM EDTA) supplemented with a protease inhibitor mix and a phosphatase inhibitor mix. The protease inhibitor mix contained a 1:100 dilution of FOCUS protease arrest (Calbiochem, USA), 5 μ g/ml E64 (Roche Diagnostics, Germany), 0.4 μ M cathepsin inhibitor III (Sigma, USA), 10 μ M MG132 (Calbiochem, USA), 20 μ M N-acetyl-leu-leu-norleu-ala (Sigma, USA) and 1 mg/ml Pefabloc[®]SC (Roche Diagnostics, Germany). The phosphatase inhibitor mix consisted of a 1:100 dilution of Phosphatase inhibitor cocktail II (Sigma, USA), 20 mM *p*-nitrophenyl phosphate, 20 mM NaF, 20 mM β -glycerophosphate, 0.2 μ M microcystin-LR (Calbiochem, USA), 0.2 μ M calyculin A (Wako, Japan), 0.2 μ M okadaic acid (Wako, Japan), 0.1 μ M phenylarsin (Sigma, USA), and 0.2 μ M cantharidin (Sigma, USA). FLAG-tagged CDC25B and mutant proteins were immunoprecipitated using FLAG M2-agarose; myc-tagged 14-3-3 proteins were immunoprecipitated with mouse monoclonal anti-myc tag antibody followed by protein G-Sepharose (Amersham Bioscience, USA). Cell lysates and immunoprecipitates were analyzed on western blots using rabbit polyclonal anti-FLAG (for CDC25B) or anti-myc antibodies (for exogenous 14-3-3), or 14-3-3 subtype-specific antibodies (for endogenous 14-3-3).

Indirect immunofluorescence microscopy

Transfected HEK293 cells grown on glass coverslips were fixed in 3.7% formaldehyde in PBS and then permeabilized with 0.5% Triton X-100 in PBS. FLAG-tagged CDC25B and mutants were detected with rabbit polyclonal anti-FLAG antibody and Alexa-594-conjugated goat anti-rabbit IgG (Molecular Probes, USA). Alternatively, myc-tagged 14-3-3 proteins were detected with mouse monoclonal anti-myc-tag antibody and Alexa-488-conjugated goat anti-mouse IgG (Molecular Probes, USA). In all samples, DNA was visualized with 4',6-diamidino-2-phenylindole (DAPI) (Sigma, USA) at 0.1 μ g/ml. To quantify the subcellular localization of CDC25B, more than 200 transfectant cells were counted and classified as having nuclear, diffuse or cytoplasmic localization.

Results

Binding of 14-3-3 β , ϵ , and σ to CDC25B

Several groups have reported the interaction of 14-3-3 isotypes, such as 14-3-3 β , ϵ , η , and ζ , with CDC25B (Mils et al., 2000; Forrest and Gabrielli, 2001). We have isolated 14-3-3 β and ϵ as proteins that interact with CDC25B in yeast two-hybrid screening (S.U., A.K., M.O., M.S., M.H., H.N., T.M., Y.I. and K.Y., unpublished data), obtaining the same results as those previously reported (Conklin et al., 1995). Apart from these two 14-3-3 proteins (β and ϵ), 14-3-3 σ was also reported to be possibly involved in a DNA damage checkpoint (Hermeking et al., 1997; Chan et al., 1999, 2000), which prompted us to isolate its cDNA and analyze its interaction with CDC25B.

We expressed FLAG-tagged CDC25B with myc-tagged 14-3-3 β , ϵ or σ in HEK293 or U2OS cells and examined their interaction (Fig. 1). Expression of these proteins was confirmed in cell extracts prepared from transfected cells, as shown in Fig.

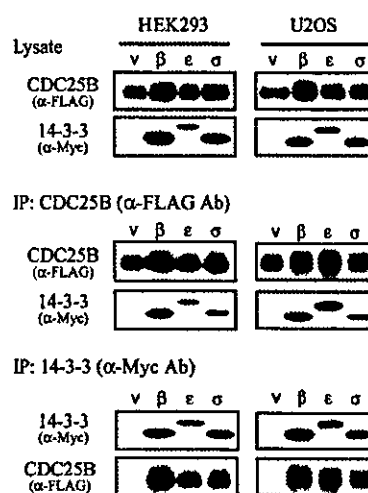


Fig. 1. 14-3-3 β , 14-3-3 ϵ , and 14-3-3 σ bind to CDC25B in transfected cells. HEK293 (left panels) or U2OS (right panels) cells were transfected with FLAG-tagged CDC25B together with either empty vector or one of the myc-tagged 14-3-3 subtypes as described in Materials and Methods. (Top row) Lysate. Expression of CDC25B and 14-3-3 subtypes was confirmed in cell lysates with anti-FLAG antibody against CDC25B or anti-myc antibody against 14-3-3, respectively. (Middle row) IP: CDC25B (α -FLAG Ab). CDC25B was immunoprecipitated with anti-FLAG beads followed by western blotting and detection with anti-FLAG antibody to detect CDC25B and anti-myc antibody to detect CDC25B-bound 14-3-3. (Bottom row) IP: 14-3-3 (α -myc Ab). Reciprocal immunoprecipitation; CDC25B was detected in anti-myc immunoprecipitates. Protein 14-3-3 subtypes were immunoprecipitated with anti-myc antibody; the collected 14-3-3 or 14-3-3-bound CDC25B was detected by immunoblotting. v, empty vector; β , 14-3-3 β ; ϵ , 14-3-3 ϵ ; σ , 14-3-3 σ .

1 (Lysate). CDC25B was immunoprecipitated with anti-FLAG beads followed by western blotting and detection with either anti-FLAG or anti-myc antibody to detect CDC25B bound to 14-3-3. The results in Fig. 1 (IP: CDC25B) clearly indicate that all three 14-3-3 proteins can bind to CDC25B in co-transfected cells. To further confirm these results, reciprocal immunoprecipitation and western blot experiments were conducted in which CDC25B was detected in anti-myc immunoprecipitates of 14-3-3 β , ϵ , or σ (Fig. 1, IP: 14-3-3). Thus, 14-3-3 σ was most probably a new CDC25B-interacting protein.

Binding site specificity of 14-3-3 subtypes

The binding of 14-3-3 proteins to target proteins requires the specific motif RSxS/T(P)xP, where S/T(P) and x represent phosphoserine or phosphothreonine, and any amino acid, respectively (Muslin et al., 1996; Yaffe et al., 1997). The arginine (R) at position -3 from the phosphorylatable serine (or threonine) is a minimal requirement. In *Xenopus* for instance, after phosphorylation of CDC25 or Wee1 by Chk1 or other kinases, 14-3-3 ϵ binds to the phosphorylated Ser287 in the RSPSMP sequence of CDC25 (Kumagai et al., 1998; Yang et al., 1999) and to the phosphorylated Ser549 in the RSVSFT sequence of Wee1 (Wang et al., 2000; Lee et al., 2001). There are several RxxS sites in CDC25B (or in our case, CDC25B1),

of which we chose the following five: 78-RRAS-81, 134-RFQS-137, 213-RPSS-216, 306-RSPS-309, and 358-RSKS-361, as shown in Fig. 2A. Of the relevant serine residues, Ser309 and Ser361 were phosphorylated by p38 in vitro and Ser309 was reported to be crucial for 14-3-3 binding after phosphorylation (Bulavin et al., 2001).

To analyze binding site specificity, we constructed three different groups of mutants in respect to the five above mentioned phosphorylatable serine sites of CDC25B1.

Members of the first group have only a single mutation that changed one phosphorylatable serine to a non-phosphorylatable alanine; these mutants were named CDC25B-S81A, S137A, etc. Members of the second group only remain a single phosphorylatable serine residue and contain mutations that changed the four serine residues to alanines; these mutants were named CDC25B-81S, 137S, etc. The only member of the last group is CDC25B-5SA in which all five serine residues were mutated to alanines. Using these mutants and the wild-type CDC25B, we determined the binding site specificity of 14-3-3 β , ϵ , and σ .

Wild-type or mutant CDC25B were co-transfected with 14-3-3 β , ϵ , or σ . Crude cell extracts were prepared, and expression of CDC25B and 14-3-3 was confirmed. Protein extracts were immunoprecipitated with anti-FLAG or anti-myc antibody, transferred for western blotting and detected with anti-myc or anti-FLAG antibody, respectively, to assess binding. We observed similar expression levels of CDC25B and 14-3-3 in transfected cells (Fig. 2B, Lysate), although lower levels of CDC25B mutants that failed to interact with 14-3-3, such as 81S and 5SA mutants, were occasionally detected (S.U., A.K., M.O., M.S., M.H., H.N., T.M., Y.I. and K.Y., unpublished data).

Interestingly, each 14-3-3 protein bound to a specific site on CDC25B (Fig. 2B, IP: CDC25B). These results clearly indicate that the CDC25B point mutation that changed Ser309 to Ala309, completely abolished 14-3-3 β binding and that mutations of the other putative binding sites had essentially no effect on binding when compared with wild-type CDC25B. Also, experiments with the CDC25B mutant containing a single phosphorylatable serine revealed that Ser309 was the

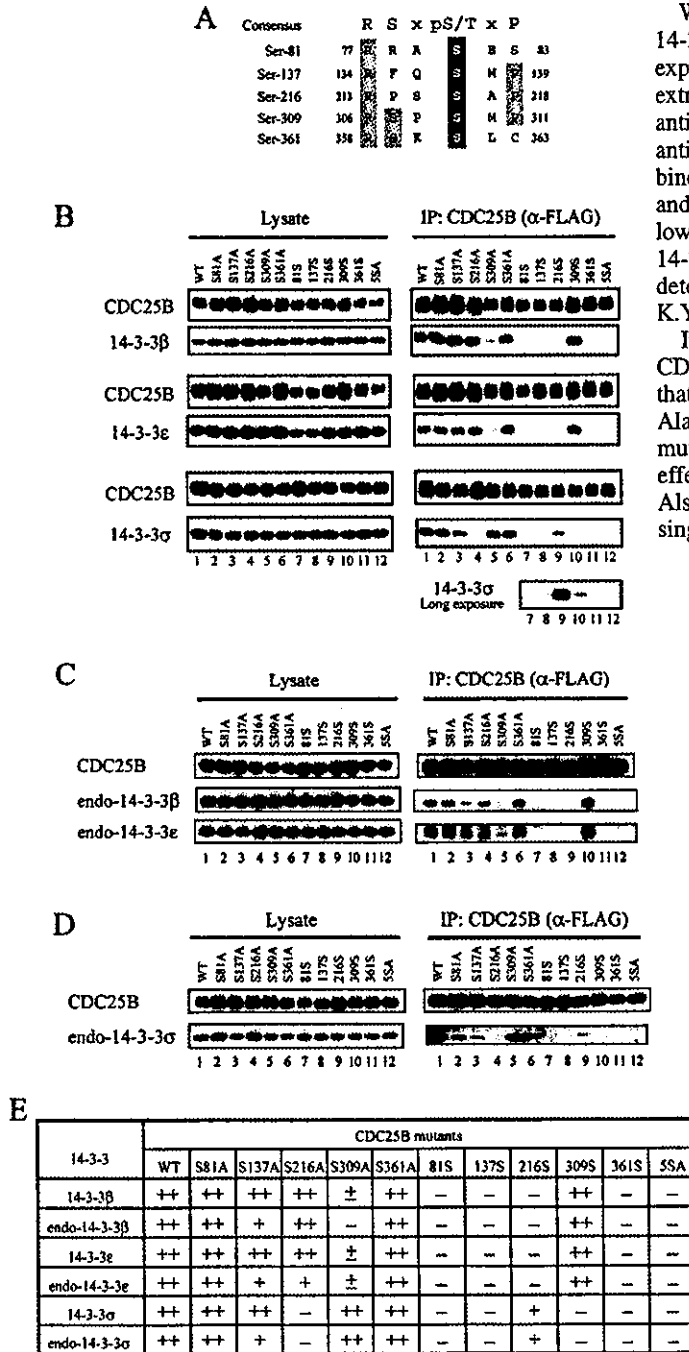


Fig. 2. Binding of 14-3-3 subtypes to CDC25B is site specific. (A) Putative 14-3-3 consensus binding sites in CDC25B. (B-D) Mutants of CDC25B were transfected into HEK293 or U2OS cells either alone or together with 14-3-3 subtypes as indicated. Recovered CDC25B proteins are indicated (upper panel of each set of figures). The letters at the top and numbers at the bottom of each blot represent the CDC25B mutants: wild-type (1); S81A (2); S137A (3); S216A (4); S309A (5); S361A (6); 81S (7); 137S (8); 216S (9); 309S (10); 361S (11); 5SA (12). The definitions of the abbreviations for each mutant are described in the text. (B) Mutants of CDC25B were co-transfected into HEK293 cells with 14-3-3 subtypes β , ϵ or σ . Protein expression was determined by immunoblot. Wild-type or mutant CDC25B proteins were immunoprecipitated with anti-FLAG beads, and CDC25B-bound 14-3-3 was determined in the lysate (Lysate) and the immunoprecipitate [IP: CDC25B (α -FLAG Ab)]. Separate panel 'long exposure' shows 14-3-3 subtype σ after an exposure for 1 hour. (C) Mutants of CDC25B were transfected into HEK293 cells. Recovered CDC25B proteins and CDC25B-bound endogenous 14-3-3 β (endo-14-3-3 β) or endogenous 14-3-3 ϵ (endo-14-3-3 ϵ) were detected with specific antibodies in the lysate (Lysate) and the immunoprecipitate [IP: CDC25B (α -FLAG Ab)]. (D) Mutants of CDC25B were transfected into U2OS cells. Recovered CDC25B and CDC25B-bound endogenous 14-3-3 σ (endo-14-3-3 σ) were detected with specific antibodies in the lysate (Lysate) and the immunoprecipitate [IP: CDC25B (α -FLAG Ab)]. (E) Binding of endogenous and transfected 14-3-3 subtypes to CDC25B mutants. ++, well bound; +, detectably bound; ±, faintly bound (could be detected only after long exposure); -, no binding.

sole site responsible for 14-3-3 β binding. A faint signal was detected with the CDC25B mutants containing Ser137 or Ser216, but only after a long exposure time (S.U., A.K., M.O., M.S., M.H., H.N., T.M., Y.I. and K.Y., unpublished data). Exactly the same results were obtained for 14-3-3 ϵ binding (Fig. 2B), i.e. the intact Ser309 fulfills the binding requirement. Surprisingly, entirely different results were obtained when 14-3-3 σ was co-expressed with CDC25B. As shown in Fig. 2B, the mutation of Ser309 to Ala309 had little effect on 14-3-3 σ binding. Instead, a single mutation changing Ser216 to Ala216 apparently abrogated the binding of 14-3-3 σ . Experiments with single-serine constructs of CDC25B provided complementary results, indicating that only Ser216 is responsible for 14-3-3 σ binding. Notice, that the amount of 14-3-3 σ that bound to the CDC25B-S216 mutant was roughly half the amount of 14-3-3 β or ϵ that bound to the CDC25B-S309 mutant. Therefore, the affinity of 14-3-3 σ for Ser216 seems to be lower than those of 14-3-3 β and ϵ for Ser309. Furthermore, 14-3-3 σ bound to two other binding sites, Ser137 and Ser309, although with a lower affinity than the binding to Ser216 (Fig. 2B, Long exposure).

Binding of endogenous 14-3-3 to CDC25B

Next, we addressed the question of whether endogenous 14-3-3 binds to transfected CDC25B. After transfection of wild-type or mutant CDC25B, CDC25B was recovered and CDC25-bound 14-3-3 β , ϵ , or σ was detected with subtype-specific antibodies. CDC25B was transfected to HEK293 cells to investigate binding of 14-3-3 β and ϵ . U2OS cells were used to determine 14-3-3 σ binding because no expression of 14-3-3 σ was detected in HEK293 cells. Binding of endogenous 14-3-3 β and ϵ is shown in Fig. 2C and that of 14-3-3 σ in Fig. 2D. As illustrated, the results were essentially the same as those for the exogenously expressed ones. 14-3-3 β and ϵ preferentially bound to Ser309 and a mutation to Ala at this site impaired 14-3-3 binding. Unlike 14-3-3 β and ϵ , a Ser to Ala mutation at Ser216 eliminated 14-3-3 σ binding (summarized in Fig. 2E). As clearly indicated, both endogenous and exogenous 14-3-3 β and ϵ preferentially bind to Ser309, whereas 14-3-3 σ prefers Ser216. Besides these two sites, Ser137 seems to be a favored binding site for the three 14-3-3 subtypes tested here because the binding signals are reduced by mutation at Ser137 (Fig. 2C and D). In respect to the other putative binding sites, we found no evidence that the 14-3-3 subtypes bind to either Ser81 or Ser361.

Multiple binding sites for 14-3-3 σ on CDC25B

The results shown in Fig. 2 suggest that 14-3-3 σ binds to CDC25B at multiple sites and possibly requires two sites to stably bind the protein. To explore this further, we constructed a series of mutants in which two serine residues were changed to alanine, and examined the binding of the 14-3-3 subtypes (Fig. 3). Compared with the single SA mutant (i.e. S216A), binding of 14-3-3 σ to double SA mutants, such as S216/309A, was weaker or absent. Further work with the double mutants indicated that either of two sites, Ser137 or Ser309, seem to work cooperatively with Ser216. These results strongly suggest that 14-3-3 σ requires two sites, Ser216 and Ser137 or Ser216 and Ser309, to interact effectively with CDC25B, and that 14-3-3 σ might function as a dimer.

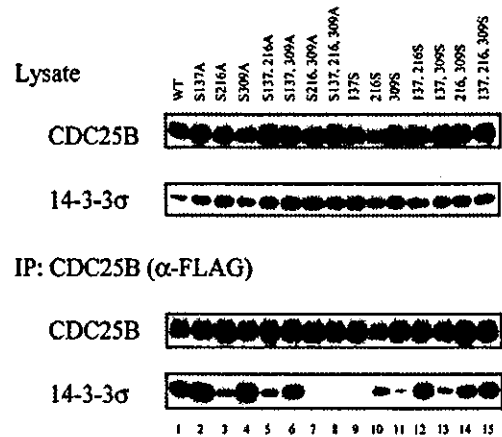


Fig. 3. Efficient binding of 14-3-3 σ to CDC25B requires two independent sites. HEK293 cells were co-transfected with 14-3-3 σ and a series of CDC25B mutants. Protein expression (Lysate) and protein binding (IP: CDC25B (α -FLAG Ab)) were detected. The letters in the upper panel of Lysate indicate CDC25B wild type and respective mutants. The definitions of the abbreviations for each mutant are described in the text.

14-3-3 binding sites and subcellular localization of CDC25B

Binding of 14-3-3 to CDC25B was previously reported to induce the redistribution of CDC25B from the nucleus to the cytoplasm; the amino acid residue essential for this effect was shown to be Ser323 of CDC25B3 (or CDC25B2), which corresponds to Ser309 of CDC25B1 in our experiments (Davezac et al., 2000; Forrest and Gabrielli, 2001). Therefore, we analyzed the subcellular localization of CDC25B mutants expressed in combination with 14-3-3 subtypes that possess different binding site preferences. To assess the effects of co-transfection on the subcellular localization of CDC25B, we distinguished three different distributions [nuclear (N), diffuse (N=C) and cytoplasmic (C)] of CDC25B (Fig. 4A). The localization of exogenously expressed CDC25B was mainly nuclear (Fig. 4B), transfected 14-3-3 β or σ was detected in the cytoplasm (S.U., A.K., M.O., M.S., M.H., H.N., T.M., Y.I. and K.Y., unpublished data). Upon co-transfection with 14-3-3 β , CDC25B exhibited a diffuse distribution (Fig. 4B). Quantitatively, the percentage of cells with nuclear CDC25B was reduced from 55% to 30% and that of cells with a diffuse distribution increased from 38% to 60% when co-expressed with 14-3-3 β . Based on our results, it is possible that nuclear localization is disturbed by 14-3-3 binding. Interestingly, the expression of 14-3-3 σ had no effect on the localization of CDC25B. These results led us to hypothesize that when 14-3-3 β binds to Ser309 of CDC25B, it can drive CDC25B from the nucleus to the cytoplasm, but that 14-3-3 σ , which does not bind primarily to Ser309, has no ability to do so.

Effects of mutations at 14-3-3 binding sites on the localization of CDC25B

The primary 14-3-3 β binding site on CDC25B was Ser309, and a point mutation at this site that changed serine to alanine abolished the interaction. If the binding of 14-3-3 β is correlated

with the cytoplasmic localization of CDC25B, 14-3-3 β could not drive the CDC25B mutant out of the nucleus. The results shown in Fig. 4C indicate that the mutation Ser309 to Ala309 in CDC25B completely disrupted its cytoplasmic localization with more than 90% of the mutant protein being located in the nuclei. In contrast to the wild type, this CDC25B mutant was not diffused into the cytoplasm by co-expression of 14-3-3 β or 14-3-3 σ . However, mutant S216A behaved like the wild type, i.e. its subcellular localization was effectively changed from nuclear to diffuse when co-expressed with 14-3-3 β (Fig. 4D). Moreover, introduction of 14-3-3 σ did not cause any change in

the distribution of CDC25B. Collectively, these results show that Ser309 is essential for the cytoplasmic distribution of CDC25B and that Ser216 does not have any influence on the subcellular localization of CDC25B, even when 14-3-3 σ binds to it.

To confirm that the subcellular distribution of CDC25B by 14-3-3 β depends on Ser309, we made mutants in which serine was changed to alanine at four of the five sites that have a single phosphorylatable serine residue. The mutants were denoted as CDC25B-81S, CDC25B-137S, CDC25B-216S, CDC25B-309S and CDC25B-361S (as mentioned in Fig. 2). These CDC25B mutants were transfected with or without 14-3-3 and their localizations analyzed. Only CDC25B-309S behaved like the wild type (Fig. 5B); the other mutants exhibited nuclear localizations, probably because they possessed the S309A mutation and could not bind to 14-3-3 β (Fig. 5A). Wild-type CDC25B and the CDC25B-309S mutant exhibited nuclear localization in about 60% of the cells (Fig. 5B). As was the case with wild-type CDC25B (see Fig. 4B), the expression of 14-3-3 β antagonized the nuclear localization of CDC25B-309S and led to a diffuse distribution (Fig. 5B). In contrast to 14-3-3 β , 14-3-3 σ did not bind to the mutant and had no effect on the nuclear localization of CDC25B-309S or wild-type CDC25B (Fig. 5B). These results strongly suggest that only Ser309 of CDC25B is required for the control of the subcellular localization of CDC25B by 14-3-3 β .

Effects of 14-3-3 ϵ on the nuclear localization of CDC25B
The results shown in Fig. 2 indicate that Ser309 of CDC25B is the specific binding site for 14-3-3 ϵ . We examined the effects

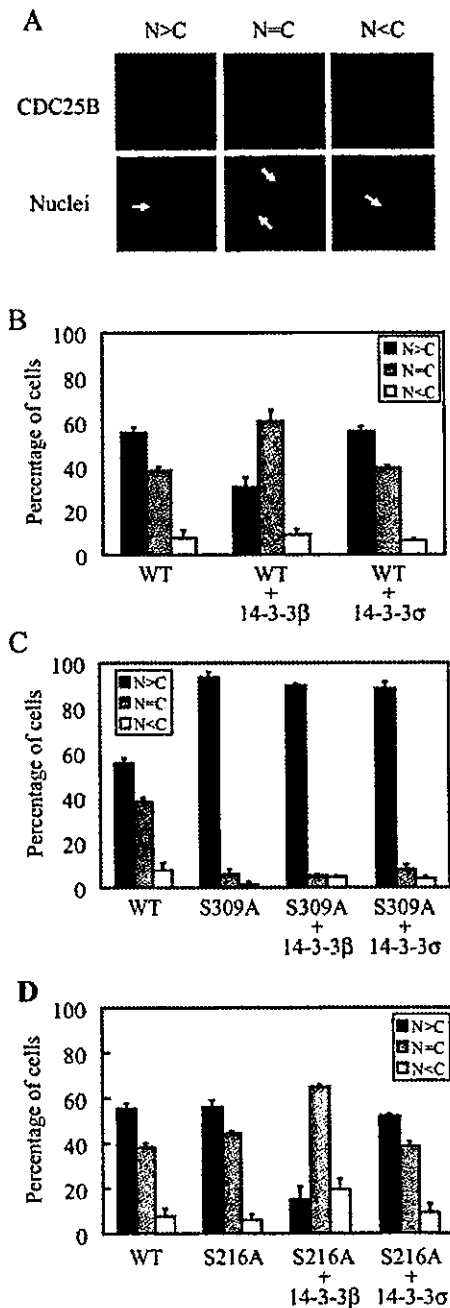


Fig. 4. 14-3-3 β but not 14-3-3 σ efficiently redistributes CDC25B from the nucleus to the cytoplasm. HEK293 cells were transfected with FLAG-tagged CDC25B in combination with empty vector, myc-tagged 14-3-3 β or myc-tagged 14-3-3 σ , followed by immunostaining with anti-FLAG antibodies to detect the subcellular localization of CDC25B and with anti-myc antibodies to detect co-transfected 14-3-3 proteins. Analyses showed that more than 95% of the cells that expressed CDC25B also expressed the co-transfected 14-3-3 proteins. (A) Exemplary images, showing how the subcellular distribution of CDC25B was evaluated: N>C, predominantly nuclear; N=C, diffuse; N<C, predominantly cytoplasmic. (B) Wild-type CDC25B was co-transfected with empty vector (WT), myc-tagged 14-3-3 β (WT+14-3-3 β) or myc-tagged 14-3-3 σ (WT+14-3-3 σ) to quantify the subcellular distribution of CDC25B. Over 200 cells expressing CDC25B were counted to determine the percentage of cells that express CDC25B with nuclear, diffuse and cytoplasmic distribution. Error bars in graphs represent the means \pm s.d. of three independent experiments. (C) Transfection with wild-type CDC25B alone (WT), S309A mutant of CDC25B alone (S309A) and mutant S309A in combination with myc-tagged 14-3-3 β (S309A+14-3-3 β) or myc-tagged 14-3-3 σ (S309A+14-3-3 σ). Over 200 cells expressing CDC25B were counted to determine the percentage of cells that express CDC25B with nuclear, diffuse and cytoplasmic distribution. Error bars in graphs represent the means \pm s.d. of three independent experiments. (D) Transfection with wild-type CDC25B alone (WT), S216A mutant of CDC25B alone (S216A) and mutant S216A in combination with myc-tagged 14-3-3 β (S216A+14-3-3 β) or myc-tagged 14-3-3 σ (S216A+14-3-3 σ). Over 200 cells expressing CDC25B were counted to determine the percentage of cells that express CDC25B with nuclear, diffuse and cytoplasmic distribution. Error bars in graphs represent the means \pm s.d. of three independent experiments.

of 14-3-3 ϵ on the subcellular localization of CDC25B in three sets of experiments. First, 14-3-3 ϵ was co-transfected with wild-type CDC25B and CDC25B-distribution (as defined above and in Fig. 4A) was analyzed by counting the cells. Co-expression of 14-3-3 ϵ reduced the percentage of cells with

nuclear localization of CDC25B from 55% to 47% and concomitantly increased the percentage of cells displaying a diffuse pattern from 40% to 55% (Fig. 6A). Second, 14-3-3 ϵ was co-transfected with the CDC25B-309S mutant. Here, the nuclear localization of CDC25B decreased from 60% to 37%, whereas its diffuse distribution increased from 35% to 55% (Fig. 6B). We found no effects of the co-expression of 14-3-3 ϵ on the subcellular localization of the CDC25B-S309A mutant (Fig. 6C). In summary, the results with 14-3-3 ϵ were exactly the same as those obtained with 14-3-3 β and different from those with 14-3-3 σ .

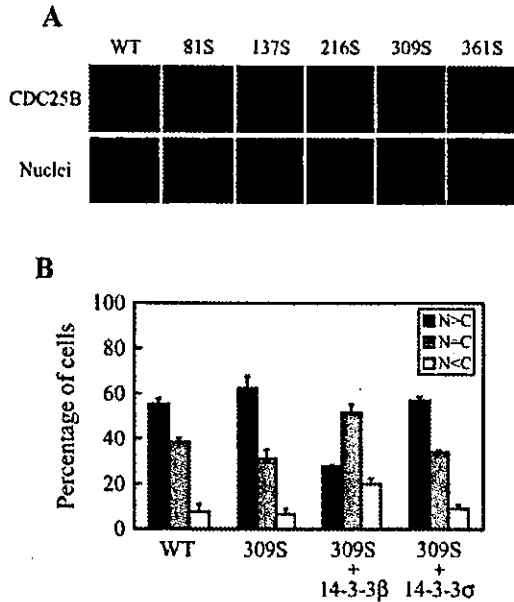


Fig. 5. Only the 309S mutant of CDC25B was distributed diffusely with co-transfection of 14-3-3 β . (A) Wild type CDC25B or different CDC25B mutants with a single phosphorylatable serine were co-transfected with 14-3-3 β into HEK293 cells. (Upper panels) Subcellular localization of CDC25B wild type and mutants. (Lower panel) Corresponding images of nuclei. (B) Percentage of cells transfected with mutant CDC25B 309S (shown in A) that express CDC25B with nuclear, diffuse and cytoplasmic distribution. Over 200 cells expressing CDC25B were counted to determine the percentage of cells that express CDC25B. Transfection with wild-type CDC25B alone (WT), 309S mutant of CDC25B alone (309S) and mutant 309S in combination with myc-tagged 14-3-3 β (309S +14-3-3 β) or myc-tagged 14-3-3 σ (309S +14-3-3 σ). Error bars in graphs represent the means \pm s.d. of three independent experiments. Subcellular distribution of CDC25B: N>C, predominantly nuclear; N=C diffuse; N<C, predominantly cytoplasmic (C).

Effects of 14-3-3 β binding on the nuclear import of CDC25B

Several previous studies demonstrated that treating cells with leptomycin B (LMB), a CRM1 (exportin1) inhibitor, disrupts the cytoplasmic localization of CDC25B (Nishi et al., 1994; Kudo et al., 1998; Karlsson et al., 1999; Davezac et al., 2000) (Fig. 7A). Therefore, it might be that 14-3-3 β -binding slows down the nuclear import of CDC25B by LMB. After transfecting CDC25B with or without 14-3-3 β , cells were treated with LMB and the nuclear accumulation of CDC25B was measured. As shown in Fig. 7B, co-expression of exogenous 14-3-3 β efficiently inhibited the nuclear import of CDC25B. Notice that this effect was not observed when 14-3-3 σ was co-transfected with CDC25B. These results suggest that 14-3-3 β masks the nuclear localizing signal (NLS) of CDC25B, which is located about 30 amino acids downstream of Ser309.

Discussion

It has long been believed that higher eukaryotic cells have two dual specificity phosphatases, CDC25B and CDC25C, which activate CDK1/cyclin B to initiate mitosis. Recent reports indicate that another dual specificity phosphatase, CDC25A, plays a crucial role in G2-M events (Mailand et al., 2002). CDC25A can bind and activate CDK1/cyclin B, and downregulation by RNAi delays mitotic entry. In addition, the overexpression of CDC25A abrogates the G2 DNA-damage checkpoint (Mailand et al., 2002; Chow et al., 2003). Therefore, it is possible to regard CDC25A as a master activator of CDK/cyclin in the cell cycle, and the roles of

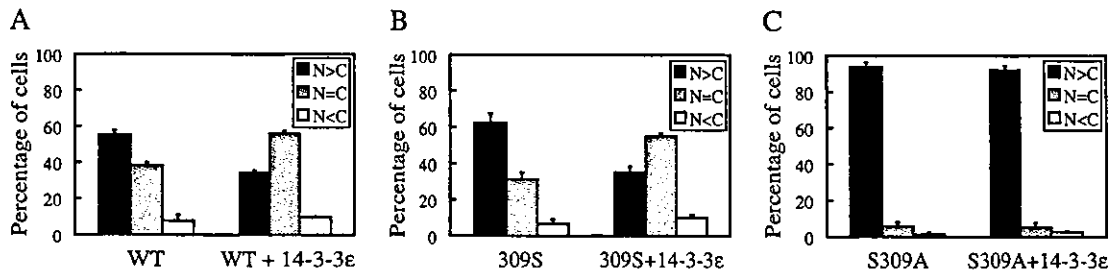
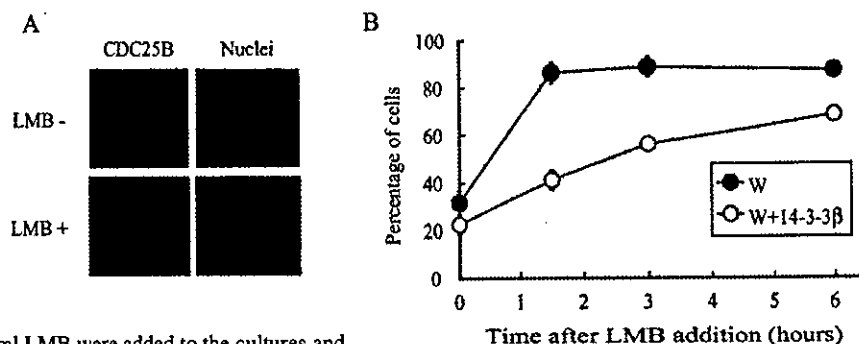


Fig. 6. 14-3-3 ϵ had effects similar to those of 14-3-3 β on the subcellular localization of CDC25B. HE293 cells were transfected with (A) wild-type CDC25B, (B) the 309S mutant or (C) the S309A mutant with or without 14-3-3 ϵ . Over 200 cells expressing CDC25B were counted to determine the percentage of cells that express CDC25B with nuclear, diffuse and cytoplasmic distribution. Error bars in graphs represent the means \pm s.d. of three independent experiments. Subcellular distribution of CDC25B: N>C, predominantly nuclear; N=C, predominantly nuclear; N<C, predominantly cytoplasmic (C).

Fig. 7. Binding of 14-3-3 β to CDC25B efficiently slowed down the nuclear import of CDC25B induced by leptomycin B (LMB). (A) HEK293 cells transfected with wild-type CDC25B and treated with 20 ng/ml LMB at for 3 hours. Transfected CDC25B was detected with anti-FLAG antibody. The upper and lower panels show the results without or with LMB treatment, respectively. (B) HEK293 cells transfected with wild-type CDC25B alone or with 14-3-3 β .



Twenty-four hours after transfection, 20 ng/ml LMB were added to the cultures and the percentage of cells exhibiting nuclear-specific localization of CDC25B was determined at the indicated time-points: 0 (before addition of LMB), 1.5, 3 or 6 hours after the addition. Over 200 cells expressing CDC25B were counted to determine the percentage of cells that express CDC25B. The percentage of cells with a nuclear localization (as shown in Fig. 4) was determined from three independent experiments. ●, CDC25B; ○, CDC25B with 14-3-3 β .

CDC25B and CDC25C as being restricted to G2-M events to activate CDK1/cyclin B.

It has been proposed that CDC25C inhibits human CDC25C, by downregulating its phosphatase activity or by binding 14-3-3 after the phosphorylation of Ser216 (Peng et al., 1997; Blasina et al., 1999; Furnari et al., 1999; Graves et al., 2001). The amount of cellular CDC25C is essentially kept constant. Therefore, a qualitative regulation of its functions, i.e. enzyme activity and subcellular localization, is required to control cell cycle progression. In the case of CDC25B, the protein accumulates as the cell cycle progresses, reaching a maximum at G2-M phase. Thus, controlling the expression of CDC25B is an effective means of regulating its function. However, at G2 phase, when the CDC25B level is at its peak, an alternate way of keeping it inactive is needed when its activation is inappropriate. Recently, several groups have reported that the binding of 14-3-3, specifically at Ser309 of CDC25B1 or Ser323 of CDC25B2 or CDC25B3, results in the cytoplasmic localization of CDC25B, supporting the theory of its redistribution from the nucleus to the cytoplasm as a critical G2-M checkpoint (Davezac et al., 2000; Forrest and Gabrielli, 2001).

In agreement with these reports, we found that 14-3-3 β and 14-3-3 ϵ bound specifically at Ser309 of CDC25B1 and that the binding effectively redistributed CDC25B, decreasing its amount in the nuclei. We consistently detected nuclear localization in about 50% of the CDC25B-transfected cells. Endogenous 14-3-3, detected with a pan-14-3-3 antibody, was recovered as a complex with exogenous CDC25B. The co-expression of 14-3-3 β or 14-3-3 ϵ reduced the nuclear localization of exogenous CDC25B by about 20%, but endogenous 14-3-3 was recovered with exogenous CDC25B. More than 95% of the introduced CDC25B was localized in nuclei when the binding of 14-3-3 was abolished by a CDC25B point mutation. Thus, it is reasonable to conclude that the binding of 14-3-3 at Ser309 of CDC25B is essential for the exclusion of CDC25B from the nucleus. We also presented evidence that binding of 14-3-3 β to CDC25B slowed down the nuclear import induced by LMB treatment. Since 14-3-3 β specifically binds to Ser309, bound 14-3-3 should impair the access of nuclear import cargos, such as importin, to the NLS.

In *Xenopus*, 14-3-3-binding to CDC25C was suggested to

mask its NLS, making its nuclear exclusion signal (NES) available for the transfer of CDC25C to the cytoplasm (Kumagai and Dunphy, 1999). The NLS in human CDC25B is located at the same position relative to the 14-3-3-binding site of CDC25C in *Xenopus*, i.e., about 30 amino acids downstream of Ser309 (Davezac et al., 2000) (S.U., A.K., M.O., M.S., M.H., H.N., T.M., Y.I. and K.Y., unpublished data). Therefore, the binding of 14-3-3 β or 14-3-3 ϵ at Ser309 could inactivate the NLS, which in turn would make the N-terminal NES dominant. This idea is further supported by the observation that the preferential binding of 14-3-3 σ to Ser216 does not cause cytoplasmic redistribution of CDC25B because Ser216 is too far away to allow 14-3-3 σ to mask the NLS. We also conclude from this result that the NES-like sequence present in the C-terminus of all 14-3-3 subtypes does not function as an NES. Thus, our results agree well with the recently presented hypothesis that the binding of 14-3-3 does not add an 'attachable NES' that targets proteins (Rittinger et al., 1999; Brunet et al., 2002). Instead, it might serve other functions, such as providing scaffolding or a cover that hides specific motifs, such as NLS or NES (Muslin and Xing, 2000; Tzivion et al., 2001; Yaffe, 2002).

Ser309 was shown to be phosphorylated by p38 MAP kinase, and the kinase activity was necessary to maintain cell cycle arrest at G2 in response to DNA damage caused by UV light (Bulavin et al., 2001). One of the checkpoint kinases, Chk1, can phosphorylate Ser309 to enhance 14-3-3-binding in vitro (Forrest and Gabrielli, 2001) (S.U., A.K., M.O., M.S., M.H., H.N., T.M., Y.I. and K.Y., unpublished data). Although co-expression of MKK6, Chk1 or Chk2 with CDC25B and 14-3-3 β enhanced the binding of 14-3-3 β to CDC25B, these effects were not significant (S.U., A.K., M.O., M.S., M.H., H.N., T.M., Y.I. and K.Y., unpublished data). Therefore, Ser309 seems to be constitutively phosphorylated, possibly by p38 or C-TAK1. If phosphorylation of this serine is crucial for the induction and/or maintenance of G2 arrest, the inactivation of the phosphatase responsible for the dephosphorylation might also occur, although enhanced checkpoint kinase activity is usually thought to maintain the phosphorylation state. The significance of the cytoplasmic localization of CDC25B in terms of cell cycle regulation, especially at the G2 checkpoint, is not clear. However, abrogation of the 14-3-3 binding site

abolished G2-arrest and thus caused localization of CDC25B to the nucleus. The overexpression of CDC25B is sufficient to override the G2 DNA damage checkpoint (Miyata et al., 2001), but in this case, Ser309 of the overexpressed CDC25B would be phosphorylated as is the endogenous residue. In addition, the amount of cellular 14-3-3 is obviously in excess of the amount of CDC25B, and thus the equilibrium between 14-3-3-bound CDC25B and unbound CDC25B should be the same in transfected cells and in normal cells. If overexpression enhances the probability of the localization of CDC25B in the nucleus, CDC25B could counteract the inhibitory effects of Wee1 kinase, leading to the activation of CDK1/cyclin B and abrogation of the G2 checkpoint. Phosphorylation of Ser309 should be necessary to inhibit premature mitosis, but it is too early to attribute maintained phosphorylation at the G2 checkpoint to the checkpoint kinases or to p38. So, if Ser309 is constantly phosphorylated, then its phosphorylation level could never be enhanced because of DNA damage (Bulavin et al., 2001). Indeed, no reports indicate a higher than normal phosphorylation level of Ser309 or Ser323 in CDC25B2 or CDC25B3 at the G2 checkpoint, although it is possible to postulate a change from the maintenance kinases to the checkpoint kinases at the checkpoint state to keep the phosphorylation level constant (Bulavin et al., 2002). Thus, the significance of the phosphorylation of Ser309, in combination with the binding of 14-3-3 at the site, must await further conclusions about the G2 checkpoint.

We have reported here the binding of 14-3-3 σ at Ser216 of CDC25B, which has not been reported previously. We have also described another site, Ser137, that seems to provide support for the binding of 14-3-3 σ . The subtypes 14-3-3 β and ϵ have little preference for either of these sites, although both serine residues partly satisfy the consensus-binding motif of 14-3-3 (RxxS). It is rare to find binding-preference differences among 14-3-3 subtypes and it should be noticed that 14-3-3 σ does not prefer Ser309 for binding even though it is in one of the typical 14-3-3 binding motifs. Interestingly, 14-3-3 σ also does not bind to CDC25C where Ser216 is located in a typical 14-3-3 binding motif (RSxSMP) (Chan et al., 1999) (S.U., A.K., M.O., M.S., M.H., H.N., T.M., Y.I. and K.Y., unpublished data). Two sites on CDC25B are required for the efficient binding of 14-3-3 σ , which means that 14-3-3 σ must be a dimer to bind efficiently to the two different sites on CDC25B.

During the preparation of this manuscript an on-line report was published, describing two sites, other than Ser323 of CDC25B2, necessary for 14-3-3 binding (Giles et al., 2003). Those two sites in CDC25B2, Ser151 and Ser230, are exactly the same as Ser137 and Ser216 of CDC25B1 that have been discussed here. We have demonstrated that 14-3-3 σ binds to these sites. It is well known that 14-3-3 σ is one of the downstream transcriptional targets of p53 (Hermeking et al., 1997). There have been several reports that 14-3-3 σ can downregulate CDK activity by binding to it or that 14-3-3 σ can move the CDK1/cyclin B complex to the cytoplasm (Bulavin et al., 2002). Here, we suggest that 14-3-3 σ downregulates the function of CDC25B and thereby acts as a G2-checkpoint regulator. Our preliminary experiments indicate that the co-expression of CDC25B and Chk1, but not MKK6 (that activates p38), enhances phosphorylation at Ser137 and Ser216 (S.U., A.K., M.O., M.S., M.H., H.N., T.M., Y.I. and K.Y.,

unpublished data). Further studies are required to determine whether the phosphorylation of both sites leads to the binding of 14-3-3 σ and to establish the consequences for CDC25B.

We thank Hiroto Okayama (University of Tokyo) and Minoru Yoshida (RIKEN) for the generous gift of CDC25B1 cDNA and leptomycin B, respectively. This work was supported in part by Grants-in-Aid for Scientific Research (to K.Y. and Y.I.) and for the Second Term of the Comprehensive 10-Year Strategy for Cancer Control (to H.N.) from the Ministry of Health, Labor, and Welfare of Japan.

References

- Blasina, A., de Weyer, I. V., Laus, M. C., Luyten, W. H., Parker, A. E. and McGowan, C. H. (1999). A human homologue of the checkpoint kinase Cds1 directly inhibits Cdc25 phosphatase. *Curr. Biol.* **9**, 1-10.
- Brunet, A., Kanai, F., Stehn, J., Xu, J., Sarbassova, D., Frangioni, J. V., Dalal, S. N., DeCaprio, J. A., Greenberg, M. E. and Yaffe, M. B. (2002). 14-3-3 transits to the nucleus and participates in dynamic nucleocytoplasmic transport. *J. Cell Biol.* **156**, 817-828.
- Bulavin, D. V., Higashimoto, Y., Popoff, I. J., Gaarde, W. A., Basrur, V., Potapova, O., Appella, E. and Fornace, A. J. Jr (2001). Initiation of a G2/M checkpoint after ultraviolet radiation requires p38 kinase. *Nature* **411**, 102-107.
- Bulavin, D. V., Amundson, S. A. and Fornace, A. J. (2002). p38 and Chk1 kinases: different conductors for the G(2)/M checkpoint symphony. *Curr. Opin. Genet. Dev.* **12**, 92-97.
- Chan, T. A., Hermeking, H., Lengauer, C., Kinzler, K. W. and Vogelstein, B. (1999). 14-3-3Sigma is required to prevent mitotic catastrophe after DNA damage. *Nature* **401**, 616-620.
- Chan, T. A., Hwang, P. M., Hermeking, H., Kinzler, K. W. and Vogelstein, B. (2000). Cooperative effects of genes controlling the G(2)/M checkpoint. *Genes Dev.* **14**, 1584-1588.
- Chow, J. P., Siu, W. Y., Fung, T. K., Chan, W. M., Lau, A., Arooz, T., Ng, C. P., Yamashita, K. and Poon, R. Y. (2003). DNA damage during the spindle-assembly checkpoint degrades CDC25A, inhibits cyclin-CDC2 complexes, and reverses cells to interphase. *Mol. Biol. Cell* **14**, 3989-4002.
- Conklin, D. S., Galaktionov, K. and Beach, D. (1995). 14-3-3 proteins associate with cdc25 phosphatases. *Proc. Natl. Acad. Sci. USA* **92**, 7892-7896.
- Davezac, N., Baldin, V., Gabrielli, B., Forrest, A., Theis-Febvre, N., Yoshida, M. and Ducommun, B. (2000). Regulation of CDC25B phosphatases subcellular localization. *Oncogene* **19**, 2179-2185.
- Ford, J. C., al-Khodairy, E., Fotou, E., Sheldrick, K. S., Griffiths, D. J. and Carr, A. M. (1994). 14-3-3 protein homologs required for the DNA damage checkpoint in fission yeast. *Science* **265**, 533-535.
- Forrest, A. and Gabrielli, B. (2001). Cdc25B activity is regulated by 14-3-3. *Oncogene* **20**, 4393-4401.
- Furnari, B., Blasina, A., Boddy, M. N., McGowan, C. H. and Russell, P. (1999). Cdc25 inhibited in vivo and in vitro by checkpoint kinases Cds1 and Chk1. *Mol. Biol. Cell* **10**, 833-845.
- Galaktionov, K. and Beach, D. (1991). Specific activation of cdc25 tyrosine phosphatases by B-type cyclins: evidence for multiple roles of mitotic cyclins. *Cell* **67**, 1181-1194.
- Galaktionov, K., Lee, A. K., Eckstein, J., Draetta, G., Meckler, J., Loda, M. and Beach, D. (1995). CDC25 phosphatases as potential human oncogenes. *Science* **269**, 1575-1577.
- Giles, N., Forrest, A. and Gabrielli, B. (2003). 14-3-3 acts as an intramolecular bridge to regulate cdc25B localization and activity. *J. Biol. Chem.* **278**, 28580-28587.
- Graves, P. R., Lovly, C. M., Uy, G. L. and Pwnica-Worms, H. (2001). Localization of human Cdc25C is regulated both by nuclear export and 14-3-3 protein binding. *Oncogene* **20**, 1839-1851.
- Hermeking, H., Lengauer, C., Polyak, K., He, T. C., Zhang, L., Thilagalingam, S., Kinzler, K. W. and Vogelstein, B. (1997). 14-3-3 sigma is a p53-regulated inhibitor of G2/M progression. *Mol. Cell* **1**, 3-11.
- Honda, R., Ohba, Y. and Yasuda, H. (1997). 14-3-3 zeta protein binds to the carboxyl half of mouse wee1 kinase. *Biochem. Biophys. Res. Commun.* **230**, 262-265.
- Hutchins, J. R., Hughes, M. and Clarke, P. R. (2000). Substrate specificity determinants of the checkpoint protein kinase Chk1. *FEBS Lett.* **466**, 91-95.

- Karlsson, C., Katich, S., Hagting, A., Hoffmann, I. and Pines, J. (1999). Cdc25B and Cdc25C differ markedly in their properties as initiators of mitosis. *J. Cell. Biol.* **146**, 573-584.
- Kudo, N., Wolff, B., Sekimoto, T., Schreiner, E. P., Yoneda, Y., Yanagida, M., Horinouchi, S. and Yoshida, M. (1998). Leptomycin B inhibition of signal-mediated nuclear export by direct binding to CRM1. *Exp. Cell Res.* **242**, 540-547.
- Kumagai, A. and Dunphy, W. G. (1999). Binding of 14-3-3 proteins and nuclear export control the intracellular localization of the mitotic inducer Cdc25. *Genes Dev.* **13**, 1067-1072.
- Kumagai, A., Yakowec, P. S. and Dunphy, W. G. (1998). 14-3-3 proteins act as negative regulators of the mitotic inducer Cdc25 in *Xenopus* egg extracts. *Mol. Biol. Cell* **9**, 345-354.
- Lammer, C., Wagerer, S., Saffrich, R., Mertens, D., Ansorge, W. and Hoffmann, I. (1998). The cdc25B phosphatase is essential for the G2/M phase transition in human cells. *J. Cell Sci.* **111**, 2445-2453.
- Lee, J., Kumagai, A. and Dunphy, W. G. (2001). Positive regulation of Wee1 by Chk1 and 14-3-3 proteins. *Mol. Biol. Cell* **12**, 551-563.
- Ma, Z. Q., Chua, S. S., DeMayo, F. J. and Tsai, S. Y. (1999). Induction of mammary gland hyperplasia in transgenic mice over-expressing human Cdc25B. *Oncogene* **18**, 4564-4576.
- Mailand, N., Podtelejnikov, A. V., Groth, A., Mann, M., Bartek, J. and Lukas, J. (2002). Regulation of G2/M events by Cdc25A through phosphorylation-dependent modulation of its stability. *EMBO J.* **21**, 5911-5920.
- Matsuoka, S., Huang, M. and Elledge, S. J. (1998). Linkage of ATM to cell cycle regulation by the Chk2 protein kinase. *Science* **282**, 1893-1897.
- Mils, V., Baldin, V., Goubin, F., Pinta, I., Papin, C., Wayne, M., Eychene, A. and Ducommun, B. (2000). Specific interaction between 14-3-3 isoforms and the human CDC25B phosphatase. *Oncogene* **19**, 1257-1265.
- Miyata, H., Doki, Y., Yamamoto, H., Kishi, K., Takemoto, H., Fujiwara, Y., Yasuda, T., Yano, M., Inoue, M., Shiozaki, H. et al. (2001). Overexpression of CDC25B overrides radiation-induced G2-M arrest and results in increased apoptosis in esophageal cancer cells. *Cancer Res.* **61**, 3188-3193.
- Morgan, D. O. (1997). Cyclin-dependent kinases: engines, clocks, and microprocessors. *Annu. Rev. Cell Dev. Biol.* **13**, 261-291.
- Muslin, A. J. and Xing, H. (2000). 14-3-3 proteins: regulation of subcellular localization by molecular interference. *Cell. Signal.* **12**, 703-709.
- Muslin, A. J., Tanner, J. W., Allen, P. M. and Shaw, A. S. (1996). Interaction of 14-3-3 with signaling proteins is mediated by the recognition of phosphoserine. *Cell* **84**, 889-897.
- Nagata, A., Igarashi, M., Jinno, S., Suto, K. and Okayama, H. (1991). An additional homolog of the fission yeast cdc25+ gene occurs in humans and is highly expressed in some cancer cells. *New Biol.* **3**, 959-968.
- Nilsson, I. and Hoffmann, I. (2000). Cell cycle regulation by the Cdc25 phosphatase family. *Prog. Cell Cycle Res.* **4**, 107-114.
- Nishi, K., Yoshida, M., Fujiwara, D., Nishikawa, M., Horinouchi, S. and Beppu, T. (1994). Leptomycin B targets a regulatory cascade of crm1, a fission yeast nuclear protein, involved in control of higher order chromosome structure and gene expression. *J. Biol. Chem.* **269**, 6320-6324.
- O'Neill, T., Giarratani, L., Chen, P., Iyer, L., Lee, C. H., Bobiak, M., Kanai, F., Zhou, B. B., Chung, J. H. and Rathbun, G. A. (2002). Determination of substrate motifs for human Chk1 and hCds1/Chk2 by the oriented peptide library approach. *J. Biol. Chem.* **277**, 16102-16115.
- Peng, C. Y., Graves, P. R., Thoma, R. S., Wu, Z., Shaw, A. S. and Piwnica-Worms, H. (1997). Mitotic and G2 checkpoint control: regulation of 14-3-3 protein binding by phosphorylation of Cdc25C on serine-216. *Science* **277**, 1501-1505.
- Peng, C. Y., Graves, P. R., Ogg, S., Thoma, R. S., Byrnes, M. J. 3rd, Wu, Z., Stephenson, M. T. and Piwnica-Worms, H. (1998). C-TAK1 protein kinase phosphorylates human Cdc25C on serine 216 and promotes 14-3-3 protein binding. *Cell Growth Differ.* **9**, 197-208.
- Rittinger, K., Budman, J., Xu, J., Volinia, S., Cantley, L. C., Smerdon, S. J., Gamblin, S. J. and Yaffe, M. B. (1999). Structural analysis of 14-3-3 phosphopeptide complexes identifies a dual role for the nuclear export signal of 14-3-3 in ligand binding. *Mol. Cell* **4**, 153-166.
- Rothblum-Oviatt, C. J., Ryan, C. E. and Piwnica-Worms, H. (2001). 14-3-3 binding regulates catalytic activity of human Wee1 kinase. *Cell Growth Differ.* **12**, 581-589.
- Sanchez, Y., Wong, C., Thoma, R. S., Richman, R., Wu, Z., Piwnica-Worms, H. and Elledge, S. J. (1997). Conservation of the Chk1 checkpoint pathway in mammals: linkage of DNA damage to Cdk regulation through Cdc25. *Science* **277**, 1497-1501.
- Sebastian, B., Kakizuka, A. and Hunter, T. (1993). Cdc25M2 activation of cyclin-dependent kinases by dephosphorylation of threonine-14 and tyrosine-15. *Proc. Natl. Acad. Sci. USA* **90**, 3521-3524.
- Tzivion, G., Shen, Y. H. and Zhu, J. (2001). 14-3-3 proteins; bringing new definitions to scaffolding. *Oncogene* **20**, 6331-6338.
- Wang, Y., Jacobs, C., Hook, K. E., Duan, H., Booher, R. N. and Sun, Y. (2000). Binding of 14-3-3beta to the carboxyl terminus of Wee1 increases Wee1 stability, kinase activity, and G2-M cell population. *Cell Growth Differ.* **11**, 211-219.
- Wang, X., Arooz, T., Siu, W. Y., Chiu, C. H., Lau, A., Yamashita, K. and Poon, R. Y. (2001). MDM2 and MDMX can interact differently with ARF and members of the p53 family. *FEBS Lett.* **490**, 202-208.
- Yaffe, M. B. (2002). How do 14-3-3 proteins work? Gatekeeper phosphorylation and the molecular anvil hypothesis. *FEBS Lett.* **513**, 53-57.
- Yaffe, M. B., Rittinger, K., Volinia, S., Caron, P. R., Aitken, A., Leffers, H., Gamblin, S. J., Smerdon, S. J. and Cantley, L. C. (1997). The structural basis for 14-3-3: phosphopeptide binding specificity. *Cell* **91**, 961-971.
- Yang, J., Winkler, K., Yoshida, M. and Kornbluth, S. (1999). Maintenance of G2 arrest in the *Xenopus* oocyte: a role for 14-3-3-mediated inhibition of Cdc25 nuclear import. *EMBO J.* **18**, 2174-2183.
- Yao, S., Slosberg, E. D., Wang, L., Hibshoosh, H., Zhang, Y. J., Xing, W. Q., Santella, R. M. and Weinstein, I. B. (1999). Increased susceptibility to carcinogen-induced mammary tumors in MMTV-Cdc25B transgenic mice. *Oncogene* **18**, 5159-5166.



Original article

Properties of anti-gp41 core structure antibodies, which compete with sera of HIV-1-infected patients

Osamu Usami ^a, Peng Xiao ^a, Hong Ling ^b, Yi Liu ^c, Tadashi Nakasone ^d, Toshio Hattori ^{a,*}

^a Division of Infectious and Respiratory Diseases, Internal Medicine, Graduate School of Medicine, Tohoku University, 1-1 Seiryō-cho, Aoba-Ku, Sendai-si, Miyagi-ken, Sendai 980-8574, Japan

^b Department of Microbiology and Parasitology, Harbin Medical University, Harbin 150086, China

^c Respiratory Department, General Airforce Hospital, Beijing, China

^d National Institute of Infectious Diseases, Tokyo 162-8640, Japan

Received 2 September 2004; accepted 5 January 2005

Abstract

To determine the correlation between the immunoreaction against the core structure of human immunodeficiency virus type (HIV-1) transmembrane protein gp41 epitopes and the disease progression, it is essential to evaluate the anti-core structure antibody epitopes and the humoral immunity against the epitopes. For this purpose we evaluated monoclonal antibodies (mAbs) against the gp41 core structure such as mAbs 50.69, 98.6 and T26, by Western blotting (WB) and flow cytometry. WB showed mAbs 50.69 and 98.6 bound to both monomeric and oligomeric gp41, and mAb T26 exclusively bound to oligomeric gp41. We evaluated the sera from *Pneumocystis pneumonia* patients (PCP; $n = 7$) and long-term survivors (LTS; $n = 7$). Competition assay with sera and mAbs for binding to H9 cells infected with HIV-1 IIIB virus was done using flow cytometry. The results revealed that PCP sera as well as LTS sera inhibited the binding of all the three mAbs, and the PCP sera inhibited mAb T26 binding more efficiently than LTS. Therefore, PCP patients retain competing immunity to antibodies against not only the shared epitopes of the core structure (binding sites of mAbs 50.69 and 98.6) but also against oligomeric gp41 specific epitope (binding site of mAb T26).

© 2005 Published by Elsevier SAS.

Keywords: HIV-1; PCP; LTS; gp41; Core structure; Sera

1. Introduction

The outcome of exposure to human immunodeficiency virus type 1 (HIV-1) is affected by humoral and cellular immune responses against HIV-1. Blocking of virus entry by antibodies is thought to be critical for vaccine development. Even though HIV-1 transmembrane protein gp41 plays a key role in both virus-mediated cell-cell infection and infection by cell-free virus, the exact conformation of the native gp41 molecule is not well known. A structural model was proposed in which fusion-active gp41 folds into a six-helix alpha-helical bundle, with three N-terminal helices forming an interior, parallel-coiled-coil trimer, while three C-terminal helices pack in the reverse direction into three hydrophobic grooves on the surface of this coiled-coil [1-3]. Two immu-

nodominant regions of gp41 core structure have been reported to define the epitopes within these regions to which infected humans respond during the course of infection [4]. The first is the region of gp41 in the vicinity of the cysteines at amino acids 598 and 604 (cluster I). The second immunogenic region position is between 644 and 663 (cluster II). Titration of sera from HIV-1-infected patients showed that there was an antibody that binds about 100-fold more efficiently to cluster I than to cluster II in the patients' sera, confirming the immunodominance of cluster I. Recently, we reported that there was an association between the clinical progression in HIV-1-infected individuals and the decline of anti-DP107 (alpha helical N-peptide) (aa 553-590) antibody, suggesting that the antibodies against the structure may have a protective role [5]. Because the DP107 peptide shows an alpha helical structure, we assumed that the humoral responses against the core structure might be associated with the clinical progression. Furuta et al. [6] showed that the DP178 (aa 638-673) peptide

* Corresponding author. Tel.: +81 22 717 8220; fax: +81 22 717 8221.

E-mail address: hattori@int1.med.tohoku.ac.jp (T. Hattori).

59 bound to gp41 and inhibits envelope protein mediated mem-
60 brane fusion. Subsequent studies by Gorny et al. have dis-
61 closed that human monoclonal antibodies (mAbs) against
62 gp41 could recognize the gp41 core structure. Among them,
63 mAb 50.69 reacts only when N51 (aa 540–590) is mixed with
64 C43 (aa 624–666), and mAb 98.6 reacts only when N36 (aa
65 546–581) is mixed with C34 (aa 628–661), and both combi-
66 nations are known to form a six-helix bundle [7,8]. The pre-
67 vious studies proved that mAb T26 binds to the epitope of a
68 six-helix bundle composed of N36 and C34 peptides [9–12]
69 (Table 1). MAbs 50.69, 98.6, T26 have an epitope that com-
70 poses the core structure so we call these mAbs anti-core struc-
71 ture mAbs because the exact antigenic structures of the native
72 and fusogenic gp41 molecule have not been clarified yet.
73 Among them, only mAb T26 has specificity to oligomeric
74 gp41 so we called mAb T26 anti-oligomeric gp41 antibody
75 because a previous study showed that mAb T26 binds spe-
76 cifically to oligomeric gp140 by immunoprecipitation [10].
77 These mAbs have been used to analyze the conformational
78 changes induced by recombinant soluble CD4 (sCD4) (Im-
79 muno. Diagnostics, Woburn, MA) because sCD4 could mimic
80 the interaction of gp120 with the cell membrane. This treat-
81 ment is known to enhance mAb 50.69 expression [13,14].
82 Such anti-core structure mAbs as 50.69, 98.6 and T26 have
83 not been studied extensively because they have less neutral-
84 izing activity [15,16], and because the gp41 core structure
85 was believed to appear only after membrane fusion occurred
86 [17]. However, to clarify the conformational properties and
87 changes of the gp41 molecule in detail, we need to evaluate
88 the binding properties of the anti-core structure mAbs, for
89 which these mAbs are useful. In the present study we were
90 able to clarify the properties of anti-gp41 mAbs.

91 Loomis-Price et al. [18] have reported that anti-gp41 immu-
92 noresponses have a more significant correlation with the dis-
93 ease progression than those of anti-gp120. It has also been
94 reported that antibodies against gp41 epitopes on HIV-1 are
95 lost or escape mutants arise and consequently control of HIV-
96 1 is lost and the virus load increases, as in the case of CDC
97 stage C [19]. Much evidence has accumulated supporting the
98 correlation with anti-gp41 immunity and disease progres-
99 sion. However, the correlation between the immunoreactions
100 against each core structure epitope and the disease progres-
101 sion remains unclear. Here, we studied the antigenicity of the

core structure, which has two immunodominant regions of
anti-gp41 antibodies, and the immunity against these epitopes
in sera of HIV-1-infected patients.

2. Materials and methods

2.1. Subjects and sera tested

We enrolled seven healthy volunteers (mean age = 33: all
of them were men) who were HIV-1 negative and whose
peripheral CD4 counts were above 500 cells per ml. And we
enrolled seven HIV-1-infected individuals (mean age = 26:
all of them were men) as LTS. LTS were defined as patients
who had not been treated with antiretroviral therapy and did
not develop AIDS-related disease for more than 10 years and
whose peripheral CD4 counts were above 500 cells per ml
(LTS) [20–22]. Sera were drawn in 1997 from six male LTS
who were hemophiliacs and estimated to have been infected
at least before 1986. Six LTS were registered in the Collabo-
rative HIV study of Japanese Natural History Committee. One
sample was drawn in 2003 for LTS #7 who been infected for
more than 10 years. And sera were drawn from seven AIDS
patients (mean age = 45) who had developed *Pneumocystis*
pneumonia (PCP) (mean CD4 count = 34) [23]. One PCP
#1 patient has been infected with HIV-1 for more than
10 years and the others were found to be infected when they
developed PCP. Six PCP patients did not have antiretroviral
therapy except PCP #2 who already had started
AZT + ddC + IDV as ART (antiretroviral therapy) when his
blood was drawn in 2003. PCP #1, #2, #3 and #6 were infected
by heterosexual intercourse and the others PCP were by homo-
sexual intercourse. In LTS #3, 5 and 6 the HIV strain was
identified as subtype B but the others were unknown (Table 2).
One male LTS #7 and one female PCP patient #1 from Tohoku
University Hospital, Division of Infectious and Respiratory
Diseases were enrolled. Sera from six male PCP patients were
kindly provided by Dr. Sato of the Sendai Medical Center.
LTS #1 and #2 sera were kindly provided by National Insti-
tute of Infectious Diseases, Tokyo, Japan. LTS #3, 4, 5 and
6 sera were kindly provided by Dr. Shin Nishihata at Ka-
goshima Seikyo Hospital. LTS #1–6 were registered in
the Collaborative HIV study of Japanese Natural History
Committee and those clinical information of LTS #1–6 was
provided from HIV Infectious Diseases Integrated Database
(<https://www.aids.nih.gov/>).

The plasma from the six PCP patients showed viral RNA
loads above 50,000 copies per ml, except case patient #2 with
3300 copies per ml. All PCP patients were hospitalized and
treated properly. Informed consent was obtained from all
patients. Plasma was separated from heparinized blood by
centrifugation and stored at –80 °C until use and thawed just
before use. Approval by the Tohoku University Ethics Com-
mittee for Clinical Investigations and informed consent were
obtained.

Table 1

Presence of different immunoreactive mAbs that bind to gp41 derived pep-
tide. Each number indicates reference
–: No binding detected between mAb and peptide. +: Significant positive
binding detected between mAb and peptide. unknown: No consensus on
whether mAb binds to peptide or not.

	C34	N36	N36/C34	C43	N51	N51/C43
50.69	– [24]	– [24]	– [24]	– [24]	– [24]	+ [24]
98.6	– [7]	– [7]	+ [7]	+ [7]	– [7]	+ [7]
T26	– [11]	– [11]	+ [11]	unknown	unknown	unknown

Table 2
Clinical characteristics of LTS (A) and PCP (B) patients

A								
Case	Age	Gender	CD4 (cells/ μ l)	Viral load (copies/ml)	ART	Subtype	Infection route	
1	20	M	648	280	Nothing	unknown	Blood Product	
2	15	M	950	950	Nothing	unknown	Blood Product	
3	34	M	665	80000	Nothing	B	Blood Product	
4	38	M	552	<400	Nothing	unknown	Blood Product	
5	32	M	501	2000	Nothing	B	Blood Product	
6	19	M	898	<400	Nothing	B	Blood Product	
7	32	M	547	<400	Nothing	unknown	unknown	
Mean	28		648	400				

B								
Case	Age	Gender	CD4 (cells/ μ l)	Viral load (copies/ml)	ART	Subtype	Infection route	
1	30	F	9	50400	Nothing	unknown	Hetero	
2	56	M	828	3300	AZT ddC IDV	unknown	Hetero	
3	60	M	212	80000	Nothing	unknown	MSM	
4	35	M	1	>100000	Nothing	unknown	Hetero	
5	32	M	34	>100000	Nothing	unknown	MSM	
6	59	M	3	>100000	Nothing	unknown	Hetero	
7	40	M	544	79000	Nothing	unknown	MSM	
Mean	45		648	400	Nothing			

153 2.2. Monoclonal antibodies

154 The anti-gp41 human mAbs 50.69, 98.6 and 246D which
155 recognize the gp41, and the biotinylated mAbs 50.69 and
156 98.6 were also kindly provided by Dr. S. Zolla-Pazner and
157 Dr. M.K. Gorny [4,24,25]. The mAb T26, which recognizes
158 the oligomeric gp41, was kindly provided by Kilgore et al.
159 [11]. The anti-gp120 mouse mAb 902, which recognizes the
160 V3 loop of gp120 [26], was provided by Dr. B. Chesebro
161 through the NIH AIDS Research/References Reagent Pro-
162 gram. MAb Chessie 8 was purified using HiTrap Protein G
163 (Amersham Biosciences, Piscataway, NJ) from Chessie
164 8 hybridoma supernatant provided by Dr. George K. Lewis
165 through the NIH AIDS Research References Reagent Pro-
166 gram.

167 2.3. Western blotting (WB)

168 Immunoassays of each mAb confirmed their binding to
169 envelope protein by LAV-BLOT1 (LOT No. 3C0175) (Bio-
170 Rad, Hercules, CA). The WB procedure was done as described
171 by the manufacturer. In brief, HIV-1 stain IIIB lysate blotted
172 membranes were washed with diluted wash solution and incu-
173 bated with diluted mAbs at 25 °C for 2 h. The membranes
174 were developed with alkaline phosphatase conjugated anti-
175 human or -mouse IgG antibody (Sigma, St. Louis, MO), fol-
176 lowed by 5-bromo-4-chlor-3-indolyl-phosphate/nitroblue-
177 terazulium reaction. The membrane images were acquired by
178 flat scanner ES-2200 (Espon, Nagano, Japan) and analyzed
179 using PhotoShop software (Adobe, San Jose, CA).

2.4. Biotinylation of antibodies

181 MABs T26 and 902 were biotinylated as follows. Ten mil-
182 ligrams biotinamidohexanoic acid *N*-hydroxysuccinimide
183 ester (Sigma) were resolved in 500 ml *N,N*-dimethy-
184 formamide (Sigma) and stocked at -20 °C. Sodium bicarbon-
185 ate was added to the stock solution to adjust the pH to 8.3.
186 One mg antibody was added to 10 ml pH adjusted solution
187 and incubated at 4 °C for overnight. Then, biotinylated mAb
188 was dialyzed with PBS 3 l at 4 °C for 24 h and detected with
189 phycoerthrin-labeled avidin (PE-avidin) (serotec Ltd.,
190 Kidlington, Oxford, UK) using flow cytometry (FACS) (Bec-
191 ton Dickinson Biosciences, San Jose, CA). Data were ana-
192 lyzed using the CellQuest software (Becton Dickinson Bio-
193 sciences).

2.5. Cell culture

195 A human T cell line, H9 cells and H9 cells infected with
196 the IIIB strain of HIV-1 (H9/IIIB) and with the MN strain of
197 HIV-1 (H9/MN) were obtained from Dr. R.C. Gallo. All cells
198 were cultured in the presence of antibiotics (penicillin and
199 streptomycin) at 37 °C in 100% humidified air containing
200 5% CO₂. The H9/IIIB and H9/MN cell lines were kept in
201 RPMI 1640 medium containing 10% fetal calf serum. The
202 viabilities of the cells were estimated using the trypan blue
203 dye exclusion method and the cells that were more than 95%
204 viable were used for the experiments. H9/IIIB and H9/MN
205 cells were proved to be infected with IIIB and MN and the
206 express the envelope protein more than 80%.

207 2.6. Sequence of HIV-1 strain analyzed

208 HTLV-III_B (GenBank accession no., X01762) and HTLV-
 209 III_{MN} (GenBank accession no., M17449) strain sequences
 210 were obtained from NIH AIDS Research and Reference
 211 Reagent program HIV-1 sequence database. Sequences were
 212 analyzed with GenetyxMAC software (Software Develop-
 213 ment, Shibuya, Japan).

214 2.7. Effect of sCD4 on the conformational changes
 215 of gp120 or gp41 by FACS

216 Conformational changes of the HIV-1 envelope glycopro-
 217 tein induced by sCD4 were detected using FACS [27]. The
 218 H9/III_B or H9/MN (5×10^5) cells were washed twice with
 219 PBS followed by incubation at 37 °C for 1 h in the absence or
 220 presence of 10 µg/ml sCD4 in RPMI 1640 medium contain-
 221 ing 0.1% BSA and 25 mM HEPES. Thereafter, the cells were
 222 washed with PBS containing 0.1% bovine serum albumin and
 223 0.01% sodium azide and incubated with anti-gp41 human or
 224 mouse mAb. The human IgG₁ (Calbiochem, La Jolla, CA)
 225 and mouse IgG myeloma proteins (R&D Systems, Minne-
 226 apolis, MN) were used as controls for the mAbs. Subse-
 227 quently, the cells were washed and detected by FITC-
 228 conjugated goat F(ab')₂ anti-mouse Ig's (FITC-aM)
 229 (Biosource, Camarillo, CA) and FITC-conjugated goat F
 230 (ab')₂ anti-human Ig's (FITC-aH) (Sigma), followed by fixa-
 231 tion with a 4% solution of formaldehyde in PBS. The fixed
 232 cells were analyzed by FACS as previously described [27].
 233 The results were obtained after subtracting the background
 234 staining of the control human or mouse IgG.

235 2.8. mAbs competition assay

236 The effects of patients' sera on the binding of biotinylated
 237 50.69, 98.6, T26 and 902 mAbs to H9/III_B (5×10^5) cells
 238 were studied. Biotinylated mAbs at saturated concentrations,
 239 50.69 (4 µg/ml), 98.6 (4 µg/ml), T26 (32 µg/ml) and 902
 240 (4 µg/ml), were added to the cells, which were pre-incubated
 241 with 20 µl sera for 1 h at 4 °C and washed twice. Cells were
 242 incubated for 30 min at 4 °C for mAb 50.69 or 98.6 and 15 min
 243 at 37 °C for mAb T26. After being washed twice, 4 µl
 244 PE-avidin was added and the cells were incubated for 30 min
 245 at 4 °C with gentle agitation and then fixed. Binding of bioti-
 246 nylated mAbs to cells was detected by FACS as above. %
 247 Inhibition by sera competition was calculated as follows. The
 248 MFI of cells incubated with healthy volunteer sera and bioti-
 249 nylated detector mAb was defined as 100% positive control.
 250 The MFI of cells without sera and detector mAb was defined
 251 as background. Background MFI was subtracted from the
 252 patient sera MFI and positive control MFI, then calculated.
 253 $[1 - (\text{patient sera MFI} - \text{background MFI}) / (\text{positive control MFI}$
 254 $- \text{background MFI})] \times 100$ (%). PCP/LTS % inhibition ratio
 255 was calculated as (% inhibition of PCP sera / % inhibition of
 256 LTS sera).

257 2.9. Statistics

258 Data are expressed as mean \pm S.E.M. One-sided nonpara-
 259 metric analysis was performed with the Mann-Whitney *U*-test
 260 to determine statistically significant differences between two
 261 groups. Differences were considered statistically significant
 262 when $P < 0.05$.

263 3. Results

264 3.1. The binding of anti-gp41 antibodies to monomeric
 265 or oligomeric gp41 molecules

266 The immunoassays of anti-gp41 antibodies binding to HIV-
 267 1 virus lysate were examined to assess whether the anti-
 268 gp41 antibodies can bind to monomeric or oligomeric
 269 gp41 molecules (Fig. 1). The mAbs 50.69, 98.6, T26, 246D,
 270 902 and Chessie 8 were added. These antibodies were detected
 271 by alkaline phosphatase conjugated anti-human or mouse anti-
 272 body. MAb 50.69, 98.6, 246D and Chessie 8 detected mono-
 273 meric gp41 as 41 kDa and oligomeric gp41 molecules as
 274 120 and 160 kDa bands, suggesting that the epitopes of these
 275 mAbs are expressed in both monomeric and oligomeric gp41.
 276 MAb T26 preferentially detected oligomeric gp41 as 120 and
 277 160 kDa bands but not monomeric gp41 as previously
 278 reported [11]. Since mAb 902 detected the band of 120 kDa
 279 gp120 but not that at 160 kDa, 160 kDa indicated the gp41 tet-
 280ramer rather than gp160 as previously reported [28]. Binding
 281 of mAb Chessie 8, which binds to the gp41 cytoplasmic linear
 282 epitope [29], to gp41 was not influenced by the gp41 con-
 283formation.

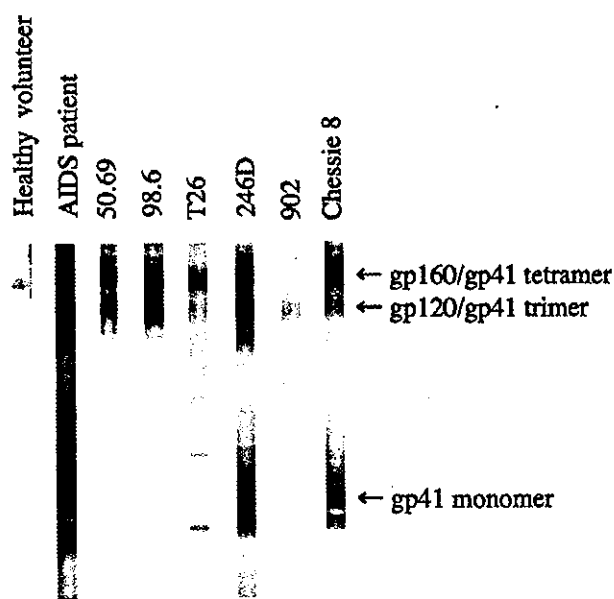


Fig. 1. WB analysis of mAbs. Each WB strip was incubated with 20 µl sera, 32 µg T26 mAb or 4 µg other mAbs diluted with 2 ml wash solution. The healthy volunteer sera as negative control and AIDS patient sera as positive control reference were performed.

284 3.2. Soluble CD4 induces the conformational change 285 of gp120 and gp41 on H9/IIIB or MN cells

286 In this study, we used sCD4 which mimicked the interac-
287 tion of cell-anchored CD4 with the HIV-1 envelope glyco-
288 protein expressed on the surface of H9/IIIB cells in a dose-
289 dependent manner and attained a maximum mAb binding at
290 10 µg/ml of sCD4 as previously described [13,14,27]. We
291 measured the change in the gp120 and gp41 epitope expo-
292 sure after the binding of sCD4 to H9/IIIB or MN cells using
293 FACS. Fig. 2a shows the binding of mAbs to H9/IIIB cells.
294 The binding of mAbs 50.69, 98.6 and 246D, gave a strong
295 signal and pretreatment of sCD4 increased the signal as fol-
296 lows: control vs. mAb 50.69 ($P = 0.046$), mAb 98.6
297 ($P = 0.032$) and mAb 246D ($P = 0.016$). The binding of mAb
298 T26 gave a weak signal and sCD4 pretreatment slightly
299 increased the signal ($P = 0.121$). The binding of mAb
300 902 gave a weak signal and sCD4 pretreatment slightly
301 decreased it ($P = 0.21$). Fig. 2b also shows the binding to
302 H9/MN cells. The binding of mAbs 50.69 and 246D gave a
303 low signal and pretreatment of sCD4 dramatically increased
304 the signal for mAb 50.69 ($P = 0.03$) and mAbs 246D
305 ($P = 0.001$). The binding of mAbs 98.6, T26 and 902 gave no
306 signal regardless of sCD4 pretreatment because there was no
307 significant difference between their MFIs and negative control
308 MFI. This result suggests that mAb 50.69 cannot bind to
309 MN strain gp41 before sCD4 pretreatment, although mAb
310 50.69 binds to activated IIIB strain gp41 on the cell surface.
311 MAb 98.6 binds to N36/C34 peptide mix or C43 peptide
312 derived from IIIB strain, but does not bind to H9/MN cells.
313 Therefore, the seven amino acids of C34, which are different
314 between the IIIB and MN strains, are possibly responsible
315 for determining whether mAb 98.6 binds to the gp41 mol-
316 ecule (Table 3).

317 3.3. PCP sera compete with anti-oligomeric gp41 antibody 318 T26 more efficiently than LTS

319 We performed a competition assay to evaluate humoral
320 immno-responses to gp41 epitopes in LTS and PCP. Fig. 3a,
321 b show the results of the competition assay between pre-
322 bound sera and anti-core structure mAbs. Biotinylated mAbs
323 were detected with PE-avidin. Biotinylated mAbs 50.69,
324 98.6 and T26 binding were significantly decreased after PCP
325 and LTS sera pretreatment for mAb 50.69 ($P = 0.00006$), mAb
326 98.6 ($P = 0.028$), mAb 902 ($P = 0.013$) and mAb T26
327 ($P = 0.0006$) after PCP sera, and for mAb 50.69 ($P = 0.0003$),
328 mAb 98.6 ($P = 0.051$), mAb T26 ($P = 0.11$) and mAb 902
329 ($P = 0.45$) after LTS sera.

330 In Fig. 3a, the average of LTS % inhibition was 52.5% for
331 mAb 50.69, 34.9% for mAb 98.6, 31.6% for mAb T26 and
332 -12.0% for mAb 902. The average of PCP % inhibition was
333 66.9% for mAb 50.69, 48.8% for mAb 98.6, 59.4% for mAb
334 T26 and -31.8% for mAb 902. PCP/LTS % inhibition ratios
335 were 1.27 for mAb 50.69, 1.39 for mAb 98.6, 1.87 for mAb
336 T26 and 2.64 for mAb 902. PCP sera blocked these mAbs

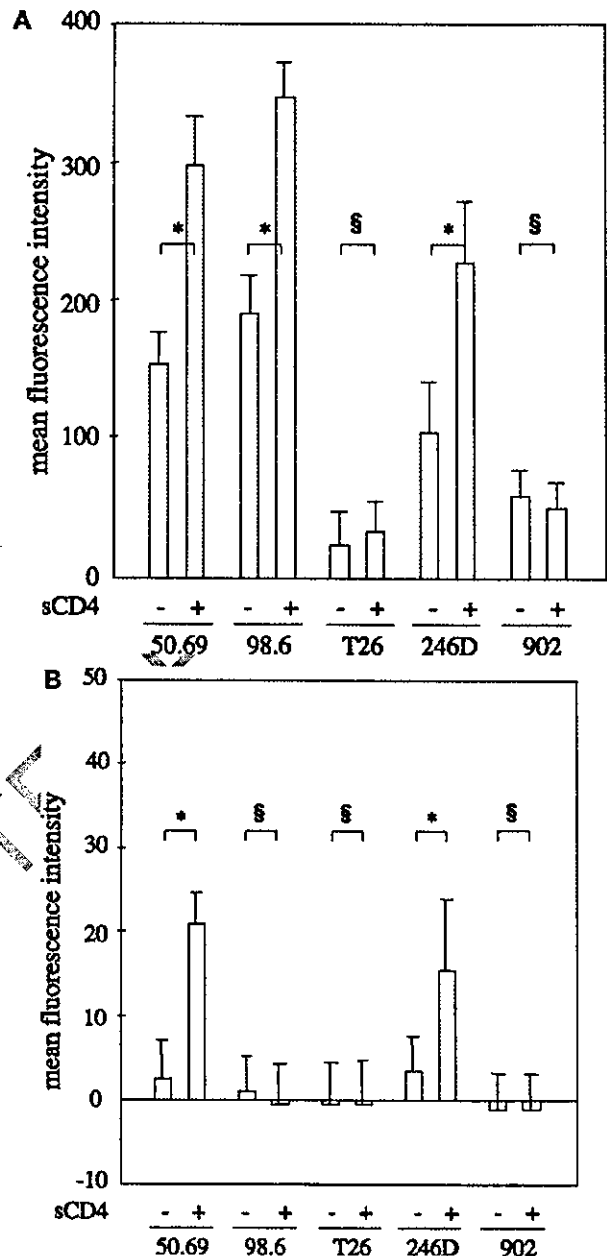


Fig. 2. Properties of mAbs binding to H9/IIIB or MN. Effect of sCD4 to env protein on (A) H9/IIIB and (B) H9/MN cells. Cells were incubated with 32 µg/ml mAb T26 and 4 µg/ml other mAbs, followed by FITC-aH or -aM incubation. Signals were detected by FL1. Each bar (\pm S.E.M.) presents the mean of triplicate determinations. * $P < 0.05$ and § $P > 0.1$ as determined by the Mann-Whitney *U*-test.

337 bindings more efficiently than LTS for mAb 50.69 ($P = 0.24$),
338 mAb 98.6 ($P = 0.54$) and mAb T26 ($P = 0.17$). This suggests
339 PCP sera contain more competitive antibody against mAbs
340 50.69, 98.6 and T26 than LTS sera. PCP sera competed with
341 mAb T26 at the same level as with mAbs 50.69 and 98.6. On
342 the other hand, anti-gp120 mAb 902 binding was enhanced
343 after PCP and LTS sera pretreatment. PCP sera pretreatment
344 more significantly enhanced mAb 902 binding to H9/IIIB cell
345 compared to LTS sera pretreatment ($P = 0.27$).

Table 3

Sequence of IIIB and MN strain gp41 N and C hapted domains

	N51	N36	DP107
IIIB :	QARQLLSGIVQQNNLRLRAEAQQLLQLTVWGIKQLQARTLAVERYLKDQ		
MN :	...L.....M.....V.....		

	C43	C34	DP178
IIIB :	NNMNTMENDREINNYTSLIHSLEESQKQKNEQELLELDKQASLWNYF		
MN :Q.E...D.....Y..L.K.T.....		

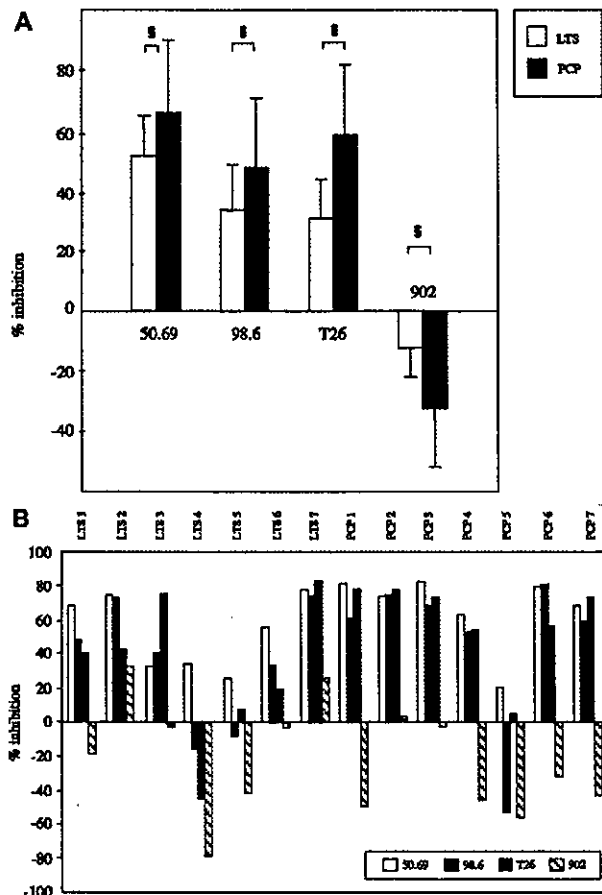


Fig. 3. % Inhibition of sera against binding of mAbs 50.69, 98.6, T26 and 902. (A) shows the average of competition between pre-bound sera and mAbs. Each bar (\pm S.E.M.) presents the mean of seven sera determinations. \S $P > 0.1$ as determined by the Mann-Whitney U -test. (B) each patient's results between pre-bound sera and mAbs.

346 4. Discussion

347 The gp41 core structure to which mAbs 50.69 and 98.6 are
 348 assumed to bind has been considered to form its unique struc-
 349 ture after receptor molecule binding. We showed that mAbs
 350 50.69 and 98.6 bind to both monomeric and oligomeric gp41,
 351 and mAb T26 binds only to oligomeric gp41 in WB. Specific
 352 recognition of the oligomeric form gp41 by mAb T26 but not
 353 by other mAbs was already described previously [10]. The
 354 difference suggests that mAbs 50.69 and 98.6 bind also to

the monomeric structure on the cell surface but mAb T26 react
 to only the oligomeric form. In FACS analysis of H9/IIIB
 cells, MFI or % of positive cells, given by mAb T26, was
 lower than by mAbs 50.69 and 98.6. This may be due to the
 fact that mAb T26 binding affinity is lower than those of mAbs
 50.69 or 98.6. But this possibility is less likely because we
 used a saturating concentration of mAb T26 in FACS. The
 low MFI of H9/IIIB cells by oligomeric specific mAb
 T26 indicated that there were only a few oligomeric struc-
 tures on H9/IIIB. It was already shown that most of the enve-
 lope structures on H9/IIIB are monomeric [30]. Further-
 more, we could not find the slightest increment of mAb
 T26 positive cells by sCD4 treatment, though mAbs 50.69 and
 98.6 reacted generally after the treatment. Therefore, not all
 the populations of gp41 on the cell surface are ready for im-
 mediate fusion even after sCD4 treatment. In fact, we found only
 1 of 10^3 – 10^4 H9/IIIB cells caused fusion in the MAGI cell
 assay (Yi Lui, unpublished observation).

We attempted to detect anti-core structure antibodies in
 HIV-1-infected sera using a competition assay of mAb
 T26 and other mAbs because mAb T26 binds specifically
 to oligomeric gp41 epitope. We used mAb 902 (anti-
 gp120 V3-IIIB virus) as a control and found that pretreatment
 by sera enhanced its binding though the cause(s) of the find-
 ing is not clear. We showed that both LTS and PCP sera con-
 tain competitive antibodies with anti-core structure mAbs.
 We could not find any distinguishable relationship between
 each patient's clinical characteristics and each competition.
 And in all LTS and PCP patients' analyses, since the % inhi-
 bition of mAb T26 in LTS and PCP was at the same level as
 that of mAb 50.69 and 98.6, LTS and PCP appear to retain
 anti-oligomeric gp41 immunity. PCP pre-bound sera com-
 peted with the anti-core structure antibodies mAbs 50.69,
 98.6, T26 more efficiently than LTS. And anti-gp41 immu-
 nity was induced more efficiently in PCP than LTS because
 PCP/LTS % inhibition ratio of mAb T26 was higher than that
 of mAbs 50.69 and 98.6 by sera competition.

It was clarified that there is the inverse correlation between
 antibody titers and disease progression when the peptide cor-
 responding to gp41 immunodominant region was used [18].
 We also described similar results using DP107 peptide [7].
 The reason why the results here were different from those of
 previous reports is not known. One reason is the specific cli-
 nical features used in this study. Excessive immunoreactive fac-
 tor in PCP lung was reported to induce developing pneumo-
 nia [31] and enhances local anti-PCP IgG production [32]. In
 addition, HIV-1 production by alveolar lymphocytes is
 increased during PCP [33]. Enhanced immunoreactions and
 higher HIV-1 copies in PCP lung possibly explain the
 enhanced production of anti HIV-1 antibodies. On the other
 hand, the reason why the increase of anti-core structure mAbs
 failed to prevent the disease progression is also unknown.
 Only few reports demonstrated neutralizing activities of these
 antibodies, probably because they recognize the final struc-
 ture and did not prevent the conformational change of
 gp41 upon virus entry [24]. Recently, we have noted one-